

High-Pressure Trickle-Bed Reactors: A Review

Muthanna H. Al-Dahhan,^{*,†} Faical Larachi,[‡] Milorad P. Dudukovic,[†] and Andre Laurent[§]

Chemical Reaction Engineering Laboratory, Department of Chemical Engineering, Washington University, Campus Box 1198, One Brookings Drive, St. Louis, Missouri 63130, Department of Chemical Engineering, Laval University & CERPIC, Québec, Canada G1K 7P4, and Laboratoire des Sciences du Génie Chimique, 1 Rue Grandville BP, 451-54001 Nancy Cedex, France

A concise review of relevant experimental observations and modeling of high-pressure trickle-bed reactors, based on recent studies, is presented. The following topics are considered: flow regime transitions, pressure drop, liquid holdup, gas–liquid interfacial area and mass-transfer coefficient, catalyst wetting efficiency, catalyst dilution with inert fines, and evaluation of trickle-bed models for liquid-limited and gas-limited reactions. The effects of high-pressure operation, which is of industrial relevance, on the physicochemical and fluid dynamic parameters are discussed. Empirical and theoretical models developed to account for the effect of high pressure on the various parameters and phenomena pertinent to the topics discussed are briefly described.

Introduction

Among the three-phase gas–liquid–solid reaction systems encountered in industrial practice, trickle-bed reactors (TBRs) are the most widely used. They are employed in petroleum, petrochemical, and chemical industries, in waste treatment, and in biochemical and electrochemical processing, as well as other applications. Table 1 lists some of the processes carried out in TBRs. The economic impact of how well these reactors operate is considerable, since in the petroleum sector alone the TBR annual processing capacity for various hydrotreatments (e.g., hydrodesulfurization, hydrocracking, hydrorefining, hydrodemetallization, hydrodenitrogenation, etc.) is estimated at ca. 1.6 billion metric tons (Trambouze, 1991). With the current market evolution toward increasing demand for light oil products, such as middle distillates, and the decreasing needs for heavy cuts, the refiners will have to keep improving their processing units for upgrading heavy oil and residual feedstocks (Trambouze, 1993). Any advance in TBR technology will thus represent substantial savings, and this stimulates the continued research efforts aimed at improving TBR operation and performance.

A trickle-bed reactor (TBR) consists of a fixed bed of catalyst particles contacted by a cocurrent downward gas–liquid flow carrying both reactants and products. When the gas and liquid are fed cocurrently upward through the catalyst bed, the system is called a flooded-bed reactor (FBR) or upflow reactor. The upflow configuration is used sparingly in industrial practice where TBRs prevail. Owing to a motionless catalyst bed, nearly plug flow is achieved in TBRs, and in that respect they are superior to other three-phase reactors where the catalyst is either slurried or fluidized. For instance, TBRs' high catalyst loading per unit volume of the liquid and low energy dissipation rate make them preferable to slurry reactors. However, the disadvantages of TBRs

are their impracticality for reactions with rapidly deactivating catalysts, such as in heavy oil hydrotreating processes, and the possibility of liquid maldistribution, which may give rise to hot spots and reactor runaway (McManus et al., 1993). The later, as shown for example by McManus et al. (1993), could be brought about by in-pore heat generated within liquid-filled catalyst pellets whence heat withdrawal is curbed by the surrounding dry conditions. In order to exploit TBR advantages in the presence of relatively slow catalyst deactivation, special reactor designs employing piston-like through-flow catalyst moving beds are used (Euzen et al., 1993).

Most commercial TBRs normally operate adiabatically at high temperatures and high pressures and generally involve hydrogen and nonwaterlike liquids with superficial gas and liquid velocities up to 30 and 1 cm/s, respectively. Kinetics and/or thermodynamics of reactions conducted in TBRs require high temperatures, which in return increase gas expansion and impede the gaseous reactant from dissolving sufficiently into the liquid. Therefore, elevated pressures (up to 30 MPa) are necessary to improve the gas solubility and the mass- and heat-transfer rates, to handle large gas volumes at less capital expense, and to slow down the catalyst deactivation which may be triggered by hydrogen starvation of the catalyst. Due to complexities associated with transport-kinetics coupling in TBRs, general scale-up and scale-down rules for the quantitative description of transport phenomena in TBRs working under realistic conditions remain elusive. This is especially true since the majority of the literature is concerned exclusively with nearly atmospheric conditions. Table 2 lists the papers on trickle-bed reactors which review various aspects of TBRs and summarize the progress in a specific area related to TBR performance. However, only the three most recent entries in Table 2 made reference to the behavior of pressurized TBRs (Gianetto and Specchia, 1992; Martinez et al., 1994; Saroha and Nigam, 1996), whereas all the others dealt with TBR research at atmospheric conditions. In view of the rapid advances that are being realized in the area of high-pressure TBRs, it is deemed appropriate to supplement the information contained in the papers referenced in Table 2 with the description of the new developments on high-pressure trickle-beds, and this is the objective of this review. Although this review

* To whom correspondence should be addressed.

[†] Washington University. Phone: (314)-935-7187, (314)-935-6021. Fax: (314)-935-4832. e-mail: muthanna@wuche.wustl.edu, dudu@wuche.wustl.edu.

[‡] Laval University. Phone: (418)-656-3566. Fax: (418)-656-5993. e-mail: flarachi@gch.ulaval.ca.

[§] Laboratoire des Sciences du Génie Chimique. Phone: 33-3-83-35-21-21. Fax: 33-3-83-32-29-75. e-mail: alaurent@ensic.u-nancy.fr.

Table 1. Some Examples of Three-Phase Reactions Carried out in Trickle-Bed Reactors

residuum and vacuum residuum desulfurization for the production of low-sulfur fuel oils (Meyers, 1996)
catalytic dewaxing of lube cuts to produce fuel or lube products for extremely cold conditions (Meyers, 1996)
sweetening of diesel, kerosene, jet fuels, heating oils (Meyers, 1996)
hydrodemetallization of residues (Trambouze, 1993; Euzen et al., 1993)
hydrocracking for production of high-quality middle-distillate fuels (Meyers, 1996)
hydrodentrification (Meyers, 1996)
isocracking for the production of isoparaffin-rich naphtha (Meyers, 1996)
production of lubricating oils (Meyers, 1996)
selective hydrogenation of butadiene to butene, of vinylacetylene to butadiene, of acetylene; of alkylanthraquinone to hydroquinone for the production of hydrogen peroxide (Charpentier, 1976; Shah, 1979)
other catalytic hydrogenations: of nitro compounds, of carbonyl compounds, of carboxylic acid to alcohols, of benzene to cyclohexane, of aniline to cyclohexylaniline, of glucose to sorbitol, of coal liquefaction extracts, of benzoic acid to hydrobenzoic acid, of caprolactone to hexanediol, of organic esters to alcohols (Germain et al., 1979)
synthesis of butynediol from acetylene and aqueous formaldehyde (Gianetto and Spechia, 1992)
immobilized enzyme reactions (Belhaj, 1984)
VOC abatement in air pollution control (Diks and Ottengraf, 1991; Chen and Chuang, 1992)
wet air oxidation of formic acid, acetic acid, and ethanol (Goto and Smith, 1975; Levec and Smith, 1976; Goto and Mabuchi, 1984; Baldi et al., 1985)
oxidation of SO ₂ (Hartman and Coughlin, 1971; Mata and Smith, 1981; Haure et al., 1990; Kiared and Zoulalian, 1992); oxidation of glucose (Tahraoui, 1990); absorption of lean CO ₂ and H ₂ S in caustic alkali solution; absorption of lean NH ₃ in an aqueous solution of H ₂ SO ₄ and H ₃ PO ₄ (Charpentier, 1976)
biochemical reactions, fermentations (Bailey and Ollis, 1986)

is not exhaustive, all the recent experimental and theoretical research on TBRs operated at elevated pressure is summarized.

The primary focus is on the developments realized during the past decade, mostly by the research groups of the University of Twente in The Netherlands, of the Chemical Reaction Engineering Laboratory at Washington University, St. Louis, MO, and of Nancy in France. The experimental conditions, the parameters measured in high-pressure TBRs, and with other relevant studies regarding high-pressure TBRs are summarized in Table 3. The following topics, in which advances have been made, will be discussed: (1) pressure effect on physicochemical properties; (2) phenomenological analysis of two-phase flow; (3) flow regime transition; (4) single-phase pressure drop; (5) two-phase pressure drop; (6) liquid holdup; (7) gas-liquid interfacial area and mass-transfer; (8) catalyst wetting efficiency; (9) catalyst dilution with inert fines in laboratory-scale high-pressure TBRs; (10) liquid-limited and gas-limited reactions in high-pressure TBRs; (11) evaluation of TBR models.

It is hoped that this paper will stimulate additional research on high-pressure trickle-bed reactors, which is needed to further advance our understanding of this reactor type, and that such research will ultimately result in more advanced fundamentally based TBR models. Professor Froment and his co-workers have advocated for many decades the fundamental approach in the description of catalytic kinetics and have succeeded in demonstrating the advantages of such an approach. A number of the catalytic chemistries that they studied have to be conducted in trickle-beds, such as hydrodesulfurization (Froment et al., 1994; Vanrysselberghe and Froment, 1996), and, hence, it is necessary to bring the TBR models to the same level that the kinetic description of the catalytic processes occurring in them has achieved. We hope that this paper will provide a motivation for such an endeavor.

1. Pressure Effect on the Fluids Physicochemical Properties

Pressure affects the physicochemical properties of gases and liquids and through this influences the fluid dynamics and transport in fixed-bed reactors. Density (ρ), molecular diffusivity (D), dynamic viscosity (μ), thermal conductivity (κ), heat capacity (C_p), surface

tension (σ), gas solubility (C^*), and Henry's constant (H) are the most sensitive to pressure. In the pressure range relevant to TBR operation, i.e., subcritical and above atmospheric conditions, it is anticipated that pressure mainly modifies the gas-phase properties, whereas the liquid remains sensitive only to temperature. Without loss of generalization, we will illustrate in what follows how hydrogen properties evolve with pressure; gases other than H₂ should, in principle, qualitatively follow similar trends. Figure 1 shows the variation of properties of H₂ in the pressure range [1–20 MPa] and a temperature around 410 K (L'Air Liquide, 1976; Sebastian et al., 1981; Reid et al., 1987). Estimation of these properties as a function of pressure is discussed in Reid et al. (1987) where a number of appropriate correlations are recommended. Apart from ρ_G , D_G , C^* , and H , the remaining properties are practically independent of pressure. Gas density increases almost proportionally to pressure (curve 1). It can also be varied by using gases of different molecular weight.

The effect of increasing pressure is to reduce the gas-side molecular diffusivity. Whether this decrease is sharp or not depends on the value of the reduced mixture temperature $T_{\text{mix},r}$ of the gas phase (Reid et al., 1987), $DP \equiv P^n$. For $T_{\text{mix},r}$ around 2.5, which is the case in our example for H₂ (curve 3), the diffusivity is inversely proportional to pressure ($n = 0$). For $T_{\text{mix},r} < 2.5$, n is less than 0, whereas n is slightly positive for $T_{\text{mix},r} > 2.5$ (Reid et al., 1987). The decrease in the mole fraction of H₂ dissolved/mole fraction of H₂ in the vapor phase with pressure (curve 5) implies that the solute (i.e., hydrogen) solubility in the liquid also increases as the solute mole fraction in the vapor phase increases. Curve 6 (mole fraction of H₂ dissolved in tetralin/H₂ partial pressure vs pressure) illustrates that the solubility of the solute increases almost linearly as the solute partial pressure increases. In summary, we can state that among the gas-phase properties which are likely to be most affected by pressure are gas density and diffusivity, gas solubility in the liquid, and Henry's constant.

2. Analysis of Two-Phase Flow Phenomena in High-Pressure TBRs

In an attempt to interpret the effect of pressure, or gas density, on the hydrodynamics of trickle beds, two types of models have been advanced. In model I,

Table 2. Articles on Trickle-Bed Reactors That Contain Reviews of Some Aspects of Trickle-Bed Operation

ref	title
Østergaard (1968)	Gas-Liquid-Particle Operations in Chemical Reaction Engineering
Satterfield (1975)	Trickle-Bed Reactors
Schwartz et al. (1976)	A New Tracer Method for Determination of Solid-Liquid Contacting Efficiency in Trickle-Bed Reactors
Van de Vusse and Wesselingh (1976)	Multiphase Reactors
Weekman (1976)	Hydroprocessing Reaction Engineering
Charpentier (1976)	Recent Progress in Two-Phase Gas-Liquid Mass Transfer in Packed Beds
Goto et al. (1977)	Trickle-Bed Oxidation Reactors
Dwivedi and Upadhyay (1977)	Particle-Fluid Mass Transfer in Fixed and Fluidized Beds
Dudukovic (1977)	Catalyst Effectiveness Factor and Contacting Efficiency in Trickle-Bed Reactors
Hofmann (1977)	Hydrodynamics, Transport Phenomena, and Mathematical Models in Trickle-Bed Reactors
Hofmann (1978)	Multiphase Catalytic Packed-Bed Reactors
Gianetto et al. (1978)	Hydrodynamics and Solid-Liquid Contacting Effectiveness in Trickle-Bed Reactors
Satterfield et al. (1978)	Liquid-Solid Mass Transfer in Packed Bed with Downward Cocurrent Gas-Liquid Flow
Specchia et al. (1978)	Solid-Liquid Mass Transfer in Cocurrent Two-Phase Flow through Packed Beds
Charpentier (1978)	Gas-Liquid Reactors
Dudukovic and Mills (1978)	Catalyst Effectiveness Factors in Trickle-Bed Reactors
Baker (1978)	Determination of the Extent of Catalyst Utilization in a Trickle-Flow Reactor
Dirkx (1979a,b)	De Trickle-Bed Reactor
Charpentier (1979)	Hydrodynamics of Two-Phase Flow Through Porous Media
Shah (1979)	Gas-Liquid-Solid Reactor Design
Van Landeghem (1980)	Multiphase Reactors: Mass Transfer and Modeling
Baldi (1981a)	Design and Scale-up of Trickle-Bed Reactors. Solid-Liquid Contacting Effectiveness
Baldi (1981b)	Heat Transfer in Gas-Liquid-Solid Reactors
Baldi (1981c)	Hydrodynamics of Multiphase Reactors
Koros (1981)	Scale-up Considerations for Mixed Phase Catalytic Reactors
Turek and Lange (1981)	Mass Transfer in Trickle-Bed Reactors at Low Reynolds Number
Morsi et al. (1981)	Hydrodynamics and Gas-Liquid-Solid Interfacial Parameters of Cocurrent Downward Two-Phase Flow in Trickle-Bed Reactors
Charpentier (1982)	What's New in Absorption with Chemical Reaction
Morsi et al. (1982)	Hydrodynamics and Interfacial Areas in Downward Cocurrent Gas-Liquid Flow through Fixed Beds. Influence of the Nature of the Liquid
Tan and Smith (1982)	A Dynamic Method for Liquid-Particle Mass Transfer in Trickle Beds
Herskowitz and Smith (1983)	Trickle-Bed Reactors: A Review
Ramachandran and Chaudhari (1983)	Three-Phase Catalytic Reactors
Crine and L'Homme (1983)	Recent Trends in the Modelling of Catalytic Trickle-Bed Reactors
Germain (1983)	Industrial Applications of Three-Phase Catalytic Fixed Bed Reactors
Hofmann (1983)	Fluid Dynamics, Mass Transfer and Chemical Reaction in Multiphase Catalytic Fixed Bed Reactors
Tarhan (1983)	Catalytic Reactor Design
Mills and Dudukovic (1984)	A Comparison of Current Models for Isothermal Trickle-Bed Reactors. Application of a Model Reaction System
Gupta (1985)	Handbook of Fluids in Motion
Rao and Drinkenburg (1985)	Solid-Liquid Mass Transfer in Packed Beds with Cocurrent Gas-Liquid Downflow
Hanika and Stanek (1986)	Operation and Design of Trickle-Bed Reactors
Dudukovic and Mills (1986)	Contacting and Hydrodynamics in Trickle-Bed Reactors
Charpentier (1986)	Mass Transfer in Fixed Bed Reactors
Gianetto and Berruti (1986)	Modelling of Trickle-Bed Reactors
Ramachandran et al. (1987)	Recent Advances in the Analysis and Design of Trickle-Bed Reactors
Ng and Chu (1987)	Trickle-Bed Reactors
Lemcoff et al. (1988)	Effectiveness Factor of Partially Wetted Catalyst Particles: Evaluation and Application to the Modeling of Trickle Bed Reactors
Zhukova et al. (1990)	Modeling and Design of Industrial Reactors with a Stationary Bed of Catalyst and Two-Phase Gas-Liquid Flow-A Review
Levec and Lakota (1992)	Liquid-Solid Mass Transfer in Packed Beds with Cocurrent Downward Two-Phase Flow
Wild et al. (1992)	Heat and Mass Transfer in Gas-Liquid-Solid Fixed Bed Reactors
Gianetto and Specchia (1992)	Trickle-Bed Reactors: State of Art and Perspectives
Martinez et al. (1994)	Three-Phase Fixed Bed Catalytic Reactors: Application to Hydrotreatment Processes
Saroha and Nigam	Trickle-Bed Reactors

changes in parameters such as liquid holdup, wetting efficiency, and gas-liquid interfacial area have been highlighted using bed-scale force considerations (Al-Dahhan and Dudukovic, 1994, 1995; Wammes and Westerterp, 1991; Wammes et al., 1991b). In model II, pore-scale force considerations have been used (Larachi et al., 1992; Lara-Marquez et al., 1992; Cassanello et al., 1996). These models can be briefly described as follows:

Model I. The effect of high pressure and gas flow rate on the energy dissipation is the central idea based on which model I is formulated. It can be used to explain the changes brought by pressure in liquid holdup, wetting efficiency, and gas-liquid interfacial area. The energy dissipation is due to the resisting frictional forces at the packing surface and the driving

forces acting on liquid flow. The driving forces consist of the pressure gradient ($\Delta P/Z$), the gas-liquid interfacial drag force ($\tau_{LG}a$), and the gravitational force ($\rho_L g$). A simple overall force balance on the gas phase shows that the pressure gradient is proportional to the gas-liquid interfacial drag; consequently, the dimensionless pressure gradient $\Delta P/\rho_L g Z$ solely determines whether liquid flow will be gravity-driven or not. The pressure gradient depends, besides the bed characteristics, on the velocities of both phases and on the physicochemical properties of the flowing fluids. As indicated in the analysis presented above, regarding the fluids physicochemical properties, mainly gas density is influenced by pressure. Thus, for given gas and liquid velocities, a higher gas density produces a higher interfacial drag force or equivalently a higher pressure gradient. The

Table 3. Studies of the High-Pressure Cocurrent Downflow and Upflow Gas-Liquid Packed-Bed Reactors

investigators	liquid/gas	bed properties	pressure (MPa)	flow rates	parameter
Abbott et al. (1967) [†]	C ₄ H ₁₀ N ₂	packing diameter (mm): 1.16 column diameter/height (mm): not given	2.41–3.79	not given	β_{hc}
Saada (1975) [†]	H ₂ O N ₂	packing diameter (mm) GB: 0.514; 0.974; 2.0640 column diameter/height (mm): 45.2/400	1.36	U _L : 0.001–0.4 U _G : 0.004–1.8	$\Delta P/Z$; β_e
Kohler and Richarz (1984, 1985) [†]	{ H ₂ O organic solution H ₂ N ₂ C ₆ H ₁₂ H ₂ O gas oil ETG N ₂	packing diameter (mm) GB: 1.5 Al ₂ O ₃ sphere and cylinder: 1.5; 3 column diameter/height (mm): 30/800 packing diameter (mm) GB: 1.3; 2; 3 column diameter/height (mm): 23/1000	1 0.1–10.1	Re _L : 0.1–8 Re _G : 0–10 L: 0.7–17 G: ≈ 0 –11	β_i ; β_s ; β_c $\Delta P/Z$; trickle-to-pulse flow transition U _{Grans} (U _L , ρ_G)
Ellman et al. (1990) [†]	biphenyl H ₂ , N ₂	Hasseni and Larachi high-pressure data + ca. 4000 atmospheric data not given	5.2 (295 °C)	Q _L : 0.6 mL/s Q _G : <10 std mL/s	$\Delta P/Z$; β_{hc} η_{CE}
Ruecker and Agkerman (1987) [†]	CH ₃ OH H ₂	packing diameter (mm) glass cylinder: 3.8 × 4.8 column diameter/height (mm): 65/500	0.2–1.2	U _L : 0.02 × 10 ⁻³ –0.15 × 10 ⁻³ U _G : 0–0.0145	β_i ; D _z
van Gelder and Westerterp (1990) [†]	H ₂ O + DEA CO ₂ + N ₂	packing size (mm) glass cylinder: 3.8 × 4.8 column diameter/height (mm): 85.5/630	0.15–1.3	U _L : 0 U _G : 0.01–0.09	k _{La} ; a; β_e
Oyevaer et al. (1989) [†]	{ EtOH H ₂ O H ₂ O + 40% ETG H ₂ O + 2 mol/L DEA H ₂ O + 1.5 mol/L DEA + 40% ETG He N ₂ + CO ₂ N ₂ + CO ₂ heavy oil + DBT H ₂	packing diameter (mm) Al ₂ O ₃ cylinder: 3.2 × 3.2 column diameter/height (mm): 51/530–2620	0.2–7.5	L: up to 7 G: up to 3	$\Delta P/Z$; β_{hc} ; β_s ; a; trickle-to-pulse & pulse-to-dispersed bubble flow U _{Grans} (U _L , ρ_G)
Wammes et al. (1990, 1991) [†]					
Ring and Missen (1991) [†]		packing diameter (mm) HDM catalyst: 2.17 column diameter/height (mm): 25/510	10 (330–370 °C) 5 (350–400 °C)	L: 0.092–0.557 G: 53 × 10 ⁻⁵ –32 × 10 ⁻⁴ L: 0.08–0.8 G: 0.003	ϵ_{Li} ; ϵ_{La} ; ϵ_{Li} ; ϵ_{Lnc} ; η_{CE}
Tsamatsoulis and Papayannakos (1994, 1995), Papayannakos et al. (1992), Thanos et al. (1996) [†]	{ sulfur-containing HVGO sulfur-free HVGO	packing size (mm) silicate sand: 0.315–0.4 ceramic extrudate: 1.1; 2.5 SiC: 0.25–2.38 glass cylinder: 2 × 4 column diameter/height (mm): 25/500			
Goto and Smith (1974) [†]	H ₂ O + HCOOH air	packing diameter (mm) 82.5% CuO and 16.5% ZnO: 0.541, 2.91 column diameter/height (mm): 25/300	4.0 (212–240 °C)	Q _L : 0.45–1.80 mL/s Q _G : <4 std mL/s	X
Levec and Smith (1976) [†]	H ₂ O + C ₃ HCOOH air	packing diameter (mm) Fe ₂ O ₃ : 0.541, 2.38 column diameter/height (mm): 25/175	6.7, 7.25 (252–286 °C)	Q _L : 0.38–1.32 mL/s Q _G : <5.9 std mL/s	X
Al-Dahhan et al. (1994, 1995, 1996), Wu et al. (1996), Khadilkar et al. (1996) [†]	{ H ₂ O H ₂ O + H ₂ O ₂ C ₆ H ₁₄ C ₆ H ₁₄ + α -methylstyrene H ₂ He N ₂	packing diameter (mm) silica shell: 1.52 Al ₂ O ₃ + 0.5% Pd cylinder: 1.57 × 4.3 Al ₂ O ₃ + 2.5% Pd cylinder: 1.3 × 5.6 GB: 1.14 silicon carbide: 0.2 trilobe: Al ₂ O ₃ + 23% CuCr: 1.3 × 5.6 column diameter/height (mm): 22/500	0.31–5	L: 0.42–5 G: 0.0033–4.03	$\Delta P/Z$; ϵ_{Lnc} ; ϵ_{La} ; η_{CE} ; X

Vergel et al. (1993, 1995) ^{†,‡}	liquid C ₄ -cut N ₂ + H ₂	0.65	L: 2.9–8.9 G: 0.17–0.53	ΔP/Z; S; X
Larachi et al. (1990, 1991, 1992, 1993, 1994), Wild et al. (1991), Lara-Marquez et al. (1992), Cassanello et al. (1996) ^{†,‡}	{ EtOH; H ₂ O H ₂ O + 1% EtOH H ₂ O + 40% C ₁₂ H ₂₂ O ₁₁ H ₂ O + 1.5 mol/L DEA PC; ETG ETG + 0.05 mol/L DEA H ₂ O + 1.5 mol/L DEA + 20% ETG H ₂ O + 1.5 mol/L DEA + 40% ETG He; N ₂ Ar; CO ₂ N ₂ + CO ₂ 1,5,9-cyclododecatriene H ₂	0.2–8.1	L: 1.4–24.5 G: ≈0.03–3	ΔP/Z; β _c ; a; k _{1a} ; trickle-to-pulse flow & flow & foaming-to-foaming pulsing U _{Grans} (U _L , ρ _G)
Stuber et al. (1996) [†]	{ packing size (mm) 0.5% Pd/Al ₂ O ₃ ; 3 × 3.2 column diameter/height (mm): 25/1500	0.1–0.4 (160–180 °C)	U _L : 3 × 10 ⁻⁴ –2 × 10 ⁻³ U _G : 0.025–0.25	X; D _z ; α _i ; k _{1a}
	{ packing diameter (mm) Al ₂ O ₃ + Pd: 2.2 column diameter/height (mm): 55; 105/1080–1560 packing diameter (mm) GB: 0.85; 1.2; 2; 3 polypropylene extrudate: 3.4 Al ₂ O ₃ sphere: 2 carbon pellet: 1.6 column diameter/height (mm): 23/400–1000			

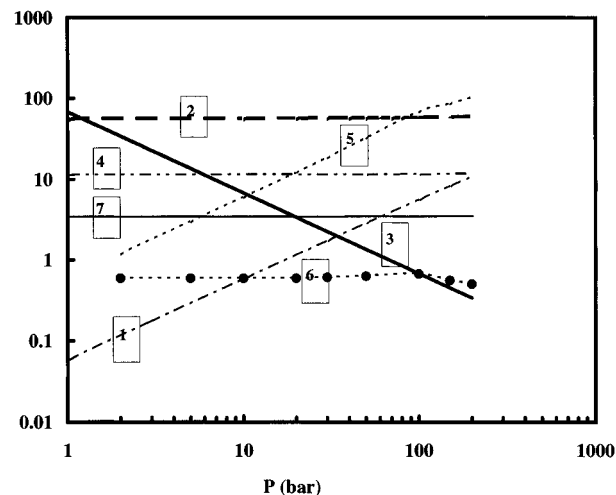


Figure 1. Influence of pressure on some characteristic properties of gaseous hydrogen. Temperature ≈ 410 K. Curve 1: density, kg/m³ (L'Air Liquide, 1976; experimental data). Curve 2: heat capacity at constant pressure, kcal/kg/K (L'Air Liquide, 1976; experimental data). Curve 3: molecular diffusivity in the gas, cm²/s (equimolecular H₂-n-C₄H₁₀) (Reid et al., 1987; correlation). Curve 4: dynamic viscosity, Pa·s $\times 10^6$ (L'Air Liquide, 1976; experimental data). Curve 5: Henry constant (mole fraction of H₂ dissolved in tetralin/mole fraction of H₂ in the vapor phase) (Sebastian et al., 1981; experimental data). Curve 6: mole fraction of H₂ dissolved in tetralin/H₂ partial pressure, bar⁻¹ $\times 10^3$ (Sebastian et al., 1981; experimental data). Curve 7: thermal conductivity cal/cm/s/K $\times 10^5$ (L'Air Liquide, 1976; experimental data).

gravitational force depends on liquid density and is not affected by pressure in the usual operating range of TBRs (≤ 30 MPa). Therefore, the effect of gas on the pressure drop can be split into an effect of the superficial gas velocity and another due to gas density. Increased gas density may result either from increased reactor operating pressure or from use of gases of higher molecular weights. In either case, increased gas density leads to increased gas-liquid interaction and higher pressure drop. Based on Al-Dahhan and Dudukovic's (1994, 1995) and Al-Dahhan's (1993) phenomenological analysis, five limiting cases can be deduced, each of which describes the effect of reactor pressure and gas superficial velocity on the pressure gradient, liquid holdup, catalyst wetting, gas-liquid interfacial area, etc. Parts a-c of Figure 2 illustrate these cases for pressure drop, liquid holdup, and catalyst wetting efficiency. The criteria (the values of the reactor pressure or gas density and superficial gas velocity) listed below that represent these cases are based on the experimental observations of Al-Dahhan and Dudukovic (1994, 1995), Larachi et al. (1990, 1992), Wammes et al. (1990a,b, 1991a,b), Lara-Marquez et al. (1992), and Cassanello et al. (1996).

Case 1: no gas flow, all pressure levels. This case corresponds to the pure trickle flow regime. While the gas is stagnant, the dimensionless pressure gradient is zero and the liquid flow is exclusively driven by its weight. Under these circumstances, reactor pressure within the range mentioned, i.e., up to 30 MPa, is not important and TBR fluid dynamics is determined by the liquid flow rate and liquid properties and by the bed characteristics. As a result, at a given liquid superficial velocity, wetting efficiency and gas-liquid interfacial area are the smallest while liquid holdup is the largest. In other words, liquid fills the major pore space readily but does not spread uniformly across the reactor diameter and over the external particles surface.

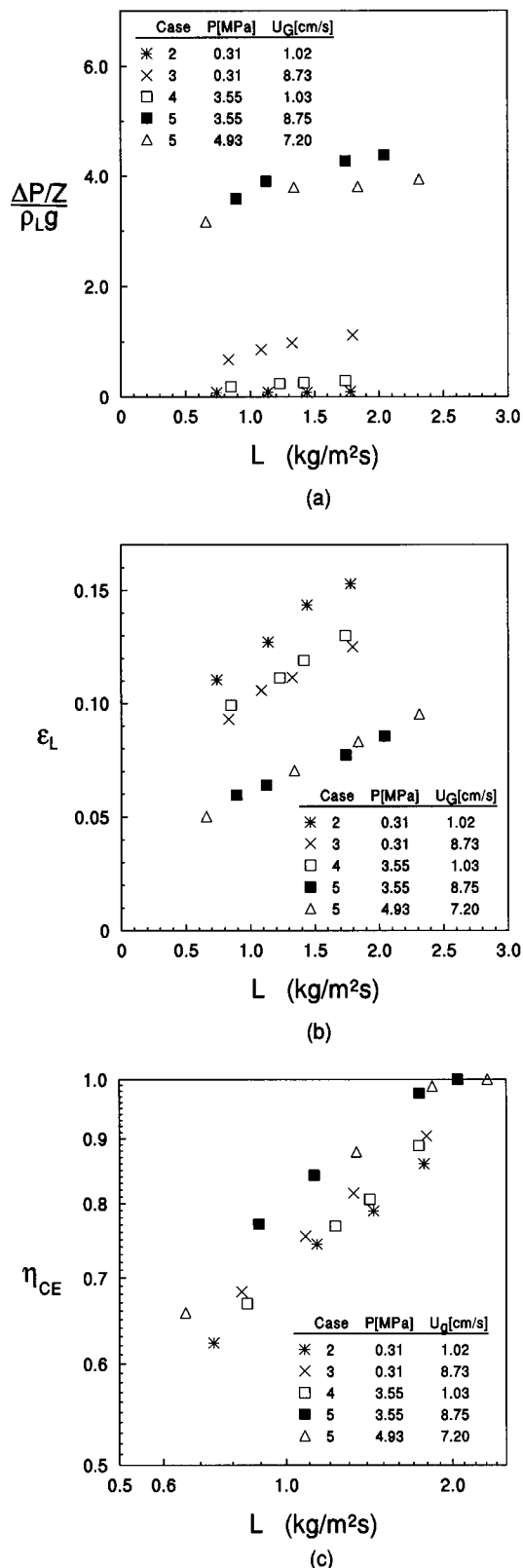


Figure 2. Effect of high pressure and gas flow rate on pressure drop (a), liquid holdup (b), and catalyst wetting efficiency (c) in a bed of extrudates: system, hexane/nitrogen; particles size, 0.157 × 0.43 cm; reactor diameter, 2.2 cm (after Al-Dahhan and Dudukovic, 1995).

Case 2: low gas superficial velocity, U_G , and low pressure, P : $U_G < 2$ cm/s and $P < 0.35$ MPa for nitrogen and for gases with equivalent density at this range of pressure. At low pressure, or nearly atmospheric pressure, and at low gas velocity the dimensionless pressure gradient changes only slightly

with pressure and gas velocity and can still be neglected. TBR fluid dynamics can to a good approximation be seen as gravity driven and gas-phase independent. This situation holds for $\Delta P/\rho_L g Z < 0.1-0.2$ (Al-Dahhan and Dudukovic, 1994, 1995; Wammes et al., 1991a,b; Wammes and Westerterp, 1990).

Case 3: high gas superficial velocity, U_G , and low pressure, P : $U_G > 7$ cm/s and $P < 0.35$ MPa for nitrogen and for gases with equivalent density at this range of pressure. Case 3 together with case 2 corresponds to the conditions at which the vast majority of experiments on TBRs have been conducted. At nearly atmospheric pressure and high gas velocity, the pressure gradient increases in comparison to the gravitational force. Consequently, the dimensionless pressure gradient ($\Delta P/\rho_L g Z$) increases, which causes a decrease in liquid holdup and an increase in the catalyst wetting efficiency and gas-liquid interfacial area. This is due to the increased gas-liquid interfacial drag, decreased liquid film, and, hence, improved liquid spreading over the external particles surface and across the reactor diameter caused by larger gas flow rate. The effects of gas flow rate in this case are more noticeable at high liquid flow rates than at lower liquid flow rates.

Case 4: low gas superficial velocity, U_G , and high pressure, P : $U_G < 2$ cm/s and $P > 3.5$ MPa for nitrogen and for gases with equivalent density at this range of pressure. As a result of increased pressure or gas density, the pressure drop increases and so does the dimensionless pressure gradient $\Delta P/\rho_L g Z$. This causes liquid holdup, wetting efficiency, and gas-liquid interfacial area to behave as in case 3 but in a less pronounced manner since the pressure gradient is more sensitive to velocity changes than to gas density changes (Al-Dahhan and Dudukovic, 1994, 1995). Nevertheless, the changes are relatively larger than those in case 2 at both low and high liquid flow rates. Case 4 arises for $\Delta P/\rho_L g Z$ larger than about 0.25 (Wammes et al., 1991b; Wammes and Westerterp, 1990; Al-Dahhan and Dudukovic, 1994, 1995).

Case 5: high gas superficial velocity, U_G , and high pressure, P : $U_G > 7$ cm/s and $P > 3.5$ MPa for nitrogen and for gases with equivalent density at this range of pressure. This is the most important case in terms of sensitivity of TBR fluid dynamics to pressure. As reactor pressure or gas density and gas flow rate increase, the dimensionless pressure gradient ($\Delta P/\rho_L g Z$) increases dramatically and liquid holdup decreases significantly. Hence, liquid film thickness at a constant liquid flow rate decreases, while the shear stress on the gas-liquid interface increases. These result in a better spreading of the liquid film over the external packing area and across the reactor diameter. Accordingly, catalyst wetting efficiency and gas-liquid interfacial area improve noticeably. The effects of high pressure and high gas velocity at high liquid flow rates are greater than those at low liquid flow rates. The trickle-to-pulse flow transition at given superficial gas velocity shifts toward higher liquid flow rate. Qualitatively, cases 3 and 4 can be viewed as the limiting cases of case 5, the first one as the limit at low pressure and the second one as the limit at low gas superficial velocity.

If the gas density is increased via molecular weight using different gases (such as helium, nitrogen, argon, carbon dioxide, etc.) at constant pressure, the effects on the fluid dynamic parameters follow the same trend of the five limiting cases discussed above. When the

pressures of gases of different molecular weights are set to result in equal densities, they bring about identical effects on the fluid dynamics as shown in Figure 5a–c (Al-Dahhan and Dudukovic, 1994; Wammes et al., 1991b, Larachi et al., 1991a, 1994).

Model II. In model II (Larachi et al., 1992; Lara-Marquez et al., 1992; Cassanello et al., 1996) it has been suggested that beyond a critical value of superficial gas velocity ($\approx 1\text{--}2$ cm/s) pressure (or gas density) intensifies the gas shear over the trickling liquid films. Below this critical velocity, pressure (or gas density) effects are marginal so that a pressurized TBR behaves as if operated at 1 atm or close to it. This operation below critical superficial gas velocity encompasses cases 1, 2, and 4 of the above-discussed model I. Above $U_G = 1\text{--}2$ cm/s the high-pressure momentum transfer through the gas–liquid interface becomes large enough to entrain the gas into the liquid. As a result the gas disperses in the liquid, forming tiny bubbles. The size of these minuscule bubbles is dictated by competition between the liquid viscous shear stress, which tends to deform and break the bubbles apart, and the force induced by interfacial tension, which tends to stabilize them. The bubbles thus formed are assumed to flow without slip with the liquid (i.e., form a pseudohomogeneous mixture with the liquid) and lead with increased gas density to enhanced gas–liquid interfacial area and gas-side and liquid-side mass-transfer coefficients. Proliferation of such small bubbles with increased gas density contributes to reduced liquid holdup and to increased $\Delta P/Z$. $\Delta P/Z$ also increases with gas density, as the bed tortuous passages render the gas flow more dissipative at higher momentum flow rates; the additional frictional interface contributed by bubbles is another factor that increases $\Delta P/Z$. The situation depicted here for $U_G > 1\text{--}2$ cm/s corresponds to case 5 of model I.

3. Flow Regime Transitions at High Pressure

Although a number of flow regimes can be identified in trickle-beds, there is a consensus to classify them all into two broad regimes, namely, a low interaction regime (LIR; trickle flow regime) and a high interaction regime (HIR, pulse, spray, bubble, and dispersed bubble flow regimes) (Charpentier and Favier, 1975; Midoux et al., 1976). The LIR is observed at low gas and liquid flow rates and is characterized by a weak gas–liquid interfacial activity and a gravity-driven liquid flow. Gas–liquid interaction in the trickle flow regime would increase at high gas and liquid flow rates and at elevated pressure (i.e., close to the transition to the HIR regimes). The liquid, which may be foaming or not, trickles down the packing in the form of droplets, films, and rivulets, while the continuous gas phase occupies the remaining porous space and flows separately. The HIR is characterized by a moderate to intense gas–liquid shear due to moderate to high flow rate of one or both of the fluids. As a result, various flow patterns arise depending on the gas-to-liquid holdup ratio and liquid tendency to foam. Low gas flow rates, and sufficiently high liquid flow rates, lead to the bubble flow regime with a continuous liquid phase which contains small spherical bubbles. At medium gas flow rates but with still high liquid flow rates, the liquid phase remains continuous but the bubbles coalesce and the gas flows in the form of elongated bubbles (Charpentier et al., 1972). This flow regime is referred to as the

dispersed bubble flow. The pulsing flow regime may be approached either from the gas-continuous trickle flow or from the liquid-continuous coalesced bubble flow regime. Such a pulsing regime is observed for moderate liquid flow rates and moderate to high gas flow rates and can be depicted as a macroscopic combination of dispersed bubble flow occurring in the liquid-rich slugs and trickle flow in the gas-rich slugs, both propagating along the bed. At still higher gas flow rates, a mist or spray flow is eventually observed for which the gas becomes again the continuous phase and in which the liquid is entrained as droplets. The above high interaction flow patterns apply for coalescing liquids, while for coalescence-inhibiting (or foaming) liquids, two more flow regimes are encountered, namely, the foaming flow and the foaming–pulsing flow (Charpentier and Favier, 1975).

In order to properly design TBRs based on laboratory data, it is important to predict in which flow regime the reactor is operating for a given set of conditions. It is also important to know if pressure effects can be well accounted for in order to predict whether the same flow regime will be preserved once scaleup or scaledown is performed. In the literature, a number of studies have been devoted to this task for which Table 2 may be consulted. Many flow regime charts and attempts at modeling flow regime transitions have been proposed thus far. Table 4 summarizes all the empirical correlations and theoretical models that have been either based or tested on high-pressure transition data. This table includes the two empirical correlations (Wammes et al., 1990a; Larachi et al., 1993a) and the three phenomenological/semitheoretical models; the predictions of all of these have been tested using high pressure transition data (Dudukovic et al., 1991; Holub et al., 1992, 1993; Dimenstein et al., 1984; Dimenstein and Ng, 1986; Ng, 1986; Ng and Chu, 1987; Sundaresan, 1987; Grosser et al., 1988; Dankworth et al., 1990a,b; Dankworth and Sundaresan, 1992). A thorough evaluation of available models and empirical correlations for the prediction of trickle-to-pulse flow transition boundaries with pressure was made by Wild et al. (1991), Larachi (1991), and Larachi et al. (1993a). These studies concluded that the use of available phenomenological and semitheoretical models for prediction of transitions at high pressure still leads to very large errors, and no single approach can be recommended.

The knowledge of several transitions which delineate the above-depicted flow regimes is indispensable in the design and scaleup of trickle-beds. Although the effect of fluid flow rates, liquid physical properties, and packing properties on the flow regime transitions has been thoroughly documented in the literature over the past 30 years (see Table 2), scarcity of measurements and prediction tools for transition boundaries at elevated pressures is noticeable. Table 3 illustrates that only three types of transitions have been studied as a function of pressure (or gas density). One was the trickle-to-pulse flow transition for nonfoaming gas–liquid systems (Hasseni et al., 1987; Wild et al., 1991; Wammes et al., 1990a,b, 1991b; Wammes and Westertep, 1991; Larachi et al., 1993a), the other was the pulsing-to-dispersed bubble flow for nonfoaming liquids (Wammes et al., 1990a), and the third was the foaming-to-foaming–pulsing transition for foaming liquids (Larachi, 1991). Moreover, only models or correlations concerned with trickle-to-pulse flow transition at high pressure were tested.

Table 4. Correlations for Prediction of Trickle-to-Pulse Flow Regime Transition in High-Pressure Trickle-Bed Reactors

author	flow configuration	P (MPa)	approach
Wammes et al. (1990a)	trickle bed	0.2–2.0	empirical
$\beta_{e,trans} = \frac{c}{U_G^{0.26} \rho_G^{0.04}} \quad c = \begin{cases} 0.27 & \text{water/N}_2 \\ 0.32 & \text{water} + 40\% \text{ ETG/N}_2 \end{cases} \quad (1)$			
tested on Talmor diagram (1977) $\frac{U_G}{U_L}$ versus $\frac{1 + \frac{1}{Fr_{GL}}}{We_{GL} + \frac{1}{Re_{GL}}}$ for water/N ₂ system			
Larachi et al. (1993a)	trickle bed	0.1–7.0	empirical
$\frac{L\lambda\psi\Phi}{G} = \left(\frac{G}{\lambda}\right)^{-1.25}$ $\lambda = \sqrt{\frac{\rho_G \rho_L}{\rho_a \rho_w}} \quad \psi = \frac{\sigma_w(\mu_L)}{\sigma_L(\mu_w)}^{1/3} \left(\frac{\rho_w}{\rho_L}\right)^{2/3} \quad \Phi = \frac{1}{4.76 + 0.5 \frac{\rho_G}{\rho_a}} \quad (2)$			
Holub et al. (1992, 1993)	trickle bed	tested on data of Wammes et al. (1990a)	semiempirical
$\frac{2.9Re_L E_1^{5/11}}{\Psi_L^{0.17} Ga_L^{0.41} Ka^{1/11}} \leq 1 \quad (3)$			
Ng (1986)	trickle bed	tested on data of Hasseni et al. (1987) and Wammes et al. (1990a)	phenomenological
$2.8 < Ga_L < 6.3 \times 10^5; 1 < \Psi_L < 55; 1.2 < L < 12 \text{ kg/m}^2\cdot\text{s}; 0.004 < G < 2.2 \text{ kg/m}^2\cdot\text{s}$			
$\frac{1}{2}\rho_G V_G^2 \left(1 - \left(\frac{d}{d_p}\right)^4\right) = 4\frac{\sigma_L}{d_p} - \frac{1}{2}\rho_L g d_p; \quad d_{p,max} = \sqrt{\frac{8\sigma_L}{\rho_L g}} \quad (4)$			
Grosser et al. (1998)	trickle bed	tested on data of Hasseni et al. (1987) and Wammes et al. (1990a)	phenomenological
$\rho_L \epsilon_L \left(\frac{\partial U_L}{\partial t} + U_L \frac{\partial U_L}{\partial z}\right) + \epsilon_L \frac{\partial P_L}{\partial z} - g\rho_L \epsilon_L - F_L(z) + \frac{\partial(\epsilon_L \mu_L^* \frac{\partial U_L}{\partial z})}{\partial z} = 0$ $\rho_G \epsilon_G \left(\frac{\partial U_G}{\partial t} + U_G \frac{\partial U_G}{\partial z}\right) + \epsilon_G \frac{\partial P_G}{\partial z} - g\rho_G \epsilon_G - F_G(z) + \frac{\partial(\epsilon_G \mu_G^* \frac{\partial U_G}{\partial z})}{\partial z} = 0$ $F_G(z) = - \left[\frac{A\mu_G(1-\epsilon)^2\epsilon^{1.8}}{d_p^2 \{\epsilon_G\}^{2.8}} + \frac{B\rho_G(1-\epsilon)\epsilon^{1.8}}{d_p \{\epsilon_G\}^{1.8}} \right] U_G - U_L \left[(U_G - U_L) \right]$ $F_L(z) = - \left[\frac{A\mu_L(1-\epsilon)^2\epsilon_L^2}{d_p^2 \epsilon^3} U_L + \frac{B\rho_L(1-\epsilon)\epsilon_L^3}{d_p \epsilon^3} U_L^2 \right] \left(\frac{\epsilon - \epsilon_{L_s}}{\epsilon_L - \epsilon_{L_s}} \right)^{2.43} - F_G(z) \quad (5)$			

From the experimental studies of the three types of flow regime boundaries at elevated pressure, the following current understanding emerges:

(a) For any range of gas density, when the pressures of gases of different molecular weights are set to have the same densities, the trickle-to-pulse flow transition occurs at the same gas and liquid superficial velocities. Thus, if a reactor is to operate at 40 MPa pure hydrogen, its trickle-to-pulse flow transition boundary can be simulated by a 1.6 MPa argon pressure for the same temperature, with the densities of argon at 1.6 MPa and hydrogen at 40 MPa being equal. Also the liquid holdup and the pressure drop keep the same values (Wammes et al., 1991b; Al-Dahhan and Dudukovic, 1994).

(b) Irrespective of the gas used, no effect of the gas density on the trickle-to-pulse flow boundary is observed as long as gas density lies below 2.3 kg/m³ as shown in Figure 3a. Hydrogen-pressurized TBRs at a few megapascals can thus be simulated by air or nitrogen at pressures close to atmospheric.

(c) At high pressures (or gas densities > 2.3 kg/m³) and high gas flow rates, the trickle-to-pulse flow transition at a given liquid (respectively gas) superficial velocity shifts toward higher gas (respectively liquid) superficial velocities, thus making the trickle flow operating region wider at elevated pressure. This enlargement of the trickle flow operating region at high pressure holds true even if, instead of drawing superficial velocity U_G versus U_L boundaries, mass superficial velocity G versus L boundaries are plotted (Figure 3) (Hasseni et al., 1987; Wild et al., 1991).

(d) At any pressure level the transition from trickling to pulsing regime occurs at smaller fluid throughputs for viscous liquids than for less viscous liquids (Figure 3b) (Wild et al., 1991).

(e) At liquid velocities corresponding to the dispersed bubble flow regime, with increasing pressure, increased gas velocities are necessary to bring pulse flow.

(f) Foaming liquids behave similarly to nonfoaming liquids in the LIR regardless of pressure. When a liquid

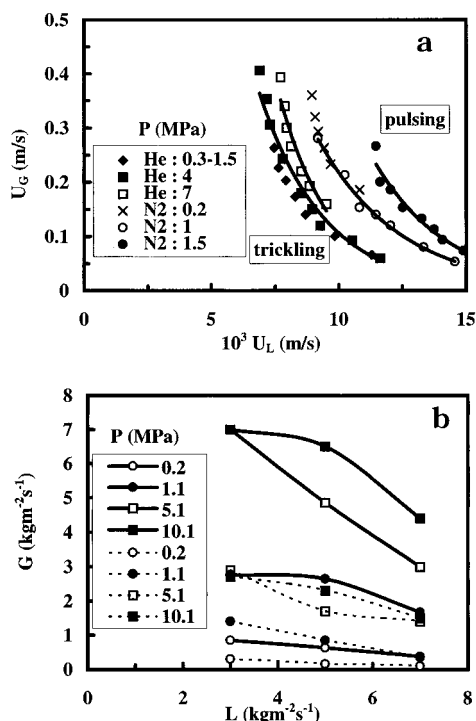


Figure 3. Effect of pressure and physical properties on trickle-to-pulse flow regime transition: (a) water/nitrogen and water/helium systems (after Wammes et al., 1991b); (b) water/nitrogen system (continuous lines) and ethyleneglycol/nitrogen system (dotted lines) (after Wild et al., 1991). Lines represent the trends.

foams at atmospheric pressure, it keeps foaming at higher pressures. In the foaming–pulsing flow regime, the foam plugs travel down the bed, with frequencies and amplitudes increasing with the gas mass flux. The amplitude in the pressure oscillations in this regime increases with pressure (Larachi, 1991). Also the gas superficial velocity corresponding to the transition between foaming and foaming–pulsing decreases as pressure increases. The inception of foaming–pulsing flow is delayed as the liquid throughput increases regardless of pressure (Larachi, 1991).

4. Single-Phase Pressure Drop

Knowledge of the single-phase pressure drop for the gas and the liquid flowing individually throughout the packed bed under high pressure conditions is important. Such information constitutes the limiting cases of TBRs operated either at trace liquid flow rates, such as in mist or deep in trickle flow regimes, or at trace gas flow rate, as in the dispersed bubble flow regime. Besides, single-phase pressure drop plays a direct role in the two-phase separated flow models developed for the quantification of liquid holdup and two-phase pressure drops in TBRs (Midoux et al., 1976; Morsi et al., 1982; Holub et al., 1992, 1993).

Single-phase pressure drop measurements have been carried out at pressures up to 18 MPa using either gases, liquids, or supercritical fluids in various bed sizes and geometries and various particle shapes and diameters (Hasseni et al., 1987; Larachi et al., 1990; Olowson and Almstedt, 1991; Salatino and Massimila, 1990; Molerus and Schweintzer, 1989; Perrut, 1987; Nakamura et al., 1985; Rowe, 1984; Rowe et al., 1984; Kawabata et al., 1981; Babu et al., 1978; Saxena and Vogel, 1976; Handley and Heggs, 1968; Simpson and Rodger, 1961). An extensive review of single-phase

pressure drops at high pressure in porous media was provided by Larachi (1991). Several gases and liquids were used, and the results were successfully represented by an Ergun-type equation (Ergun, 1952). Pressure, density, and molecular weight, which primarily affect the fluid inertia, are well accounted for by the Reynolds number. Analysis of the Blake–Kozeny–Carman h_K and Burke–Plummer h_B coefficients (which are known as Ergun constants E_1 and E_2 , respectively) showed no evidence of clear dependence upon pressure or gas or liquid density (Hasseni et al., 1987; Larachi et al., 1990; Al-Dahhan, 1993). However, h_K (E_1) values were slightly different depending on whether the working fluid was a liquid or a gas.

5. Two-Phase Pressure Drop

The influence of pressure on the two-phase pressure drop in trickle-beds was first studied by Hasseni et al. (1987). Operating pressures extending from atmospheric pressure up to 10.1 MPa using nitrogen allowed pressure drops to be obtained in both the trickle flow and pulse flow and at their corresponding transition. Wammes et al. (1990a,b, 1991a,b) and Wammes and Westerterp (1990, 1991) measured the pressure drops at pressures up to 7.5 MPa in the trickling, pulsing, bubbly dispersed flow regimes and trickling/pulsing and pulsing/bubbly dispersed transitions. Larachi et al. (1991a, 1990) and Wild et al. (1991) conducted extensive experiments (over 1500 measurements) on the effect of pressure (from 0.2 to 8.1 MPa) by testing more than 30 systems. Experiments were performed using pure or mixed gases and pure or mixed aqueous or organic solutions. These latter systems were chosen to explore behaviors such as foaming, coalescing, viscous nonfoaming, and viscous foaming flows. The operating conditions covered trickling, pulsing, bubbly dispersed regime, foaming pulsing regime, and their respective transition boundaries. Recently, Al-Dahhan (1993) and Al-Dahhan and Dudukovic (1994) measured two-phase pressure drops in the trickling flow regime using organic and aqueous nonfoaming liquids at pressures up to 5.0 MPa (see Figure 2a). The pressure dependence of the two-phase pressure drop was discussed in light of the five limiting cases of model I described above. Tables 3 and 5 summarize the experimental conditions explored and the empirical correlations and theoretical models proposed so far by the different investigators, respectively. Al-Dahhan and Dudukovic (1994) showed that Holub et al.'s (1992, 1993) phenomenological model predicts both pressure drop and liquid holdup better than the current empirical high-pressure correlations for the range of operating conditions studied. Al-Dahhan et al. (1996) extended this model to improve its prediction at high pressure and high gas flow rates by accounting for the gas–liquid interactions.

Figures 2a and 4a–d illustrate some of the experimental data at high-pressure operation. The five limiting cases discussed in section 2 describe well the experimental observations as shown in Figure 2a. When the pressures of gases of different molecular weights are set to have equal densities at constant liquid throughputs, they bring about identical pressure drops as illustrated in Figure 5a,c (Al-Dahhan and Dudukovic, 1994; Wammes et al., 1991b, Larachi et al., 1991a, 1994) for the case of He at 2.1 MPa and N₂ at 0.3 MPa which have the same density.

It is noteworthy that for coalescing to weakly foaming systems and gases of sufficient inertia, i.e., $\rho_G U_G^2 \geq 1\%$

Table 5. Correlations and Models for Prediction of Two-Phase Pressure Drop in High-Pressure Trickle- and Flooded-Bed Reactors

author	flow configuration	P (MPa)	approach
Ellman et al. (1988) high interaction regime	trickle bed	0.1–10.1	empirical
$f = A(X_G \xi_1)^j + B(X_G \xi_1)^k \text{ where } \xi_1 = \frac{Re_L^{0.25} We_L^{0.2}}{(1 + 3.17 Re_L^{1.65} We_L^{1.2})^{0.1}}$			
low interaction regime			
$f = C(X_G \xi_2)^m + D(X_G \xi_2)^n \text{ where } \xi_2 = \frac{Re_L^2}{0.001 + Re_L^{1.5}}$			
$A = 6.96; B = 53.27; C = 200; D = 85; j = -2; k = -1.5; m = -1.2; n = -0.5 \quad (6)$			
Wammes et al. (1991b)	trickle bed	0.2–7.5	empirical
$\frac{\Delta P}{Z} \frac{d_p}{\frac{1}{2} \rho_G U_G^2} = 155 \frac{1 - \epsilon}{\epsilon_G} \left(\frac{\rho_G U_G d_p \epsilon}{\mu_G (1 - \epsilon)} \right)^{-0.37} \quad (7)$			
Larachi et al. (1991a)	trickle bed	0.2–8.1	empirical
$f = \frac{1}{(X_G (Re_L We_L)^{1/4})^{3/2}} \left[31.3 + \frac{17.3}{\sqrt{X_G (Re_L We_L)^{1/4}}} \right] \quad (8)$			
Larachi et al. (1994)	flooded bed	0.1–5.1	empirical
$f = \frac{1}{(X_G (Re_L We_L)^{1/4})^{3/2}} \left[45.6 + \frac{15.9}{\sqrt{X_G (Re_L We_L)^{1/4}}} \right] \quad (9)$			
Holub et al. (1992, 1993), Al-Dahhan and Dudukovic (1994)	trickle bed	0.31–5	phenomenological
$\Psi_L = \frac{\Delta P}{\rho_L g Z} + 1 = \left(\frac{\epsilon}{\epsilon_L} \right)^3 \left[\frac{E_1 \bar{Re}_L}{(1 - \epsilon) G a_L} + \frac{E_2 \bar{Re}_L^2}{(1 - \epsilon)^2 G a_L} \right]$			
$\Psi_G = \frac{\Delta P}{\rho_G g Z} + 1 = \left(\frac{\epsilon}{\epsilon - \epsilon_L} \right)^3 \left[\frac{E_1 \bar{Re}_G}{(1 - \epsilon) G a_G} + \frac{E_2 \bar{Re}_G^2}{(1 - \epsilon)^2 G a_G} \right]$			
$\Psi_L = 1 + \frac{\rho_G}{\rho_L} (\Psi_G - 1) \quad (10)$			

^a E_1 and E_2 are Ergun constants that characterize the bed and are determined from single-phase flow measurements. The third equation is first solved for liquid holdup, and then the first or the second equation is solved for pressure drop.

$\rho_L U_L^2$, it was found (Larachi et al., 1990, 1991a, 1994; Wild et al., 1991) that the gas momentum rate can be used as a similarity criterion to evaluate pressure drops at high-pressure operation from atmospheric pressure drop experiments. Thus, if the flow regime is controlled by inertia and the liquid mass flux is the same,

$$[\rho_G U_G^2 = G^2 / \rho_G]_{1 \text{ atm}} = [\rho_G U_G^2 = G^2 / \rho_G]_{P > 1 \text{ atm}}$$

then

$$[\Delta P / Z]_{1 \text{ atm}} = [\Delta P / Z]_{P > 1 \text{ atm}}$$

This is demonstrated by Figure 4d, in which a plot of pressure gradient to gas inertia ratio as a function of gas momentum rate is able to merge all pressure gradient lines at four different gas densities (Figure 4c) and a unique line describes pressure drop irrespective of gas density.

6. Liquid Holdup

Liquid holdup plays an important role in TBR hydrodynamics and mass and heat transfer. In highly exothermic reactions, knowledge of holdup is essential for avoiding hot spots and for preventing reactor run-

away. Liquid holdup also affects the catalyst wetting efficiency, which, in turn, affects the reaction selectivity depending on whether the reaction takes place solely on the wetted catalyst area or on dry and wetted catalyst areas alike. Table 3 presents the experimental conditions explored by the various investigators, whereas the correlations and models devoted to liquid holdup are listed in Table 6. Figures 2b and 6 present some of the experimental data for liquid holdup at high-pressure operation. The phenomenological analysis of Al-Dahhan and Dudukovic (1994), presented in section 2, describes well the effect of pressure and gas flow rates on liquid holdup. Systems with gases of different molecular weights that are maintained at the same densities, by adjusting the reactor pressure, render the same liquid holdup and pressure drop at the same liquid mass flux as illustrated in Figure 5b. Hence, increasing gas density via molecular weight by using different gases (helium, nitrogen, argon, carbon dioxide) at constant pressure duplicates the trends due to pressure (Al-Dahhan and Dudukovic, 1994; Wammes et al., 1991b, Larachi et al., 1991a, 1994). The static liquid holdup measured by the stop-flow technique was found not to be affected by the reactor pressure and gas flow rate (Al-Dahhan, 1993; Al-Dahhan and Dudukovic, 1994; Wammes, 1990; Wammes et al., 1991a).

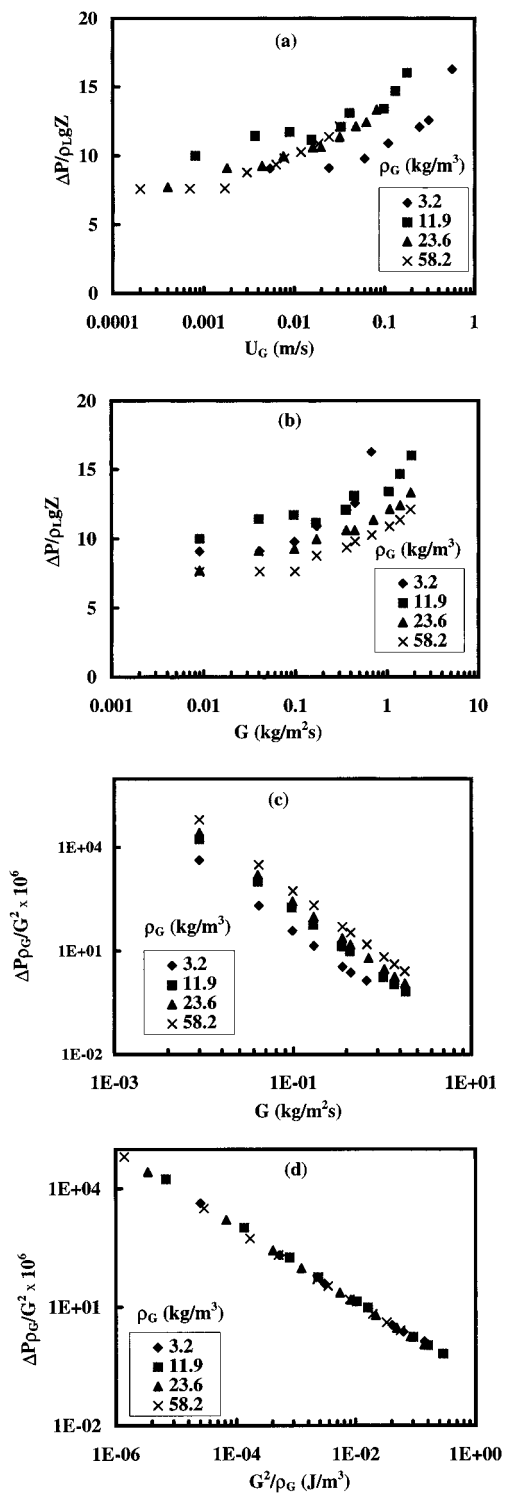


Figure 4. Effect of gas density on the two-phase pressure gradient: (a) pressure gradient-to-liquid gravitational force ratio as a function of superficial gas velocity; (b) pressure gradient-to-liquid gravitational force ratio as a function of gas mass flux; (c) pressure drop-to-gas inertia force ratio as a function of gas mass flux; (d) pressure drop-to-gas inertia force ratio as a function of gas momentum flow rate. System: ethylene glycol/nitrogen. $L = 13.2 \text{ kg/m}^2\cdot\text{s}$. Particles: 2 mm glass beads. Reactor diameter: 2.3 cm (after Larachi, 1991).

Liquid holdup at high pressure was first reported by Abbott et al. (1979), who measured liquefied butane holdup under nitrogen pressure in the range 2.4–3.8 MPa. Larkins-type correlations (Larkins et al., 1961), involving the Lockhart–Martinelli dimensionless number (Lockhart and Martinelli, 1949) successfully described their data. Later, by means of a tracer injection

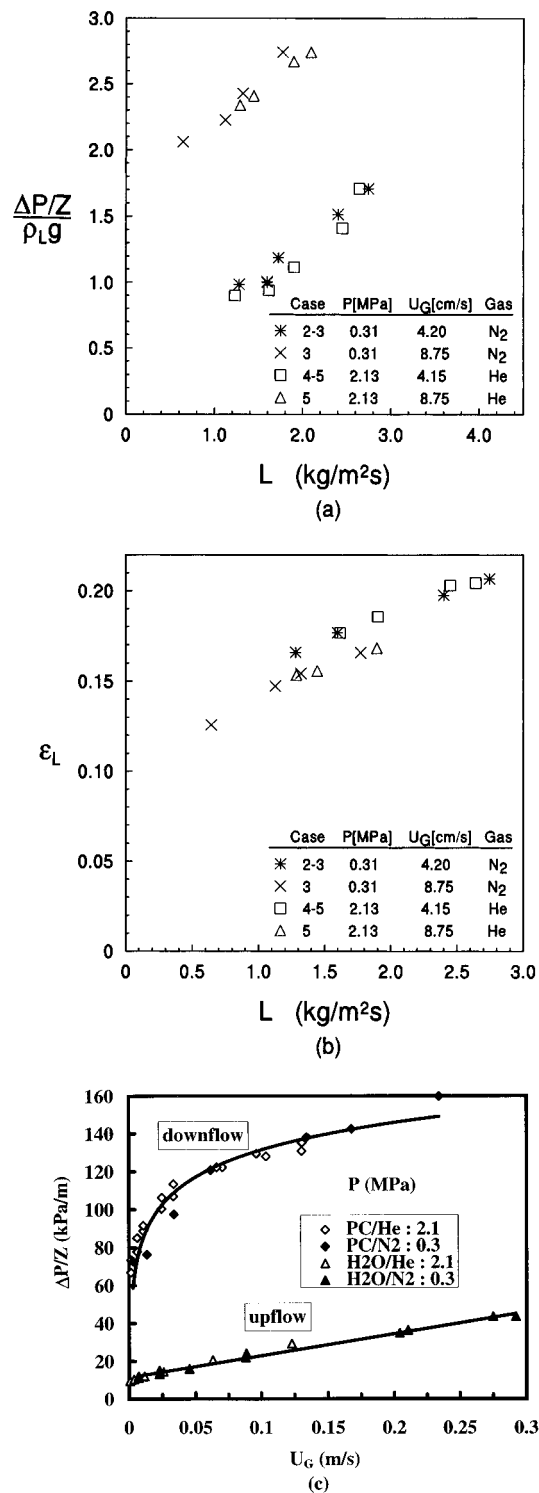


Figure 5. Effect of gas density on pressure drop (a) and liquid holdup (b) in trickle-bed reactors after Al-Dahhan and Dudukovic (1994). System: hexane/nitrogen and helium. Particles: 1.14 mm glass beads. Reactor diameter: 2.2 cm (a) after Larachi et al. (1994) for trickle-bed and upflow reactors. For cocurrent downflow (TBR): system, polypropylene carbonate (PC)/nitrogen and helium; particles, 1.4 mm glass beads; reactor diameter, 2.3 cm. For cocurrent upflow: system, water/nitrogen and helium; particles, 3.4 mm polypropylene extrudates; reactor diameter, 2.3 cm. Lines represent the trends.

technique, Kohler and Richarz (1984, 1985) measured capillary (static) and total liquid holdups up to 1 MPa. Water, nonviscous coalescing organic solutions, nitrogen, and hydrogen were the test fluids used within the operating range restricted to the trickle flow regime up to the transition to pulsing. Under zero gas flow and

Table 6. Correlations and Models for Prediction of Liquid Holdup in High-Pressure Trickle- and Flooded-Bed Reactors

author	flow configuration	P (MPa)	approach
Abbott et al. (1967)	trickle bed	2.41–3.79	empirical
$\log_{10}(\beta_{nc}) = -0.44 + 0.40\log_{10}(\chi) - 0.12(\log_{10}(\chi))^2 \quad (11)$			
Saada (1975)	flooded bed	1.36	empirical
$\beta_e = c \left(\frac{Re_L}{Re_G} \right)^d$ $\left(\frac{c}{d} \right) = \begin{pmatrix} 0.48 \\ 0.25 \end{pmatrix} \quad \text{if } Re_G < 0.44 Re_L^2 \left(\frac{d_p}{D_c} \right)^{0.38}$ $\left(\frac{c}{d} \right) = \begin{pmatrix} 0.32 \\ 0.07 \end{pmatrix} \quad \text{if } Re_G > 0.44 Re_L^2 \left(\frac{d_p}{D_c} \right)^{0.38} \quad (12)$			
Kohler and Richarz (1985)	trickle bed	0.1–1.0	empirical
$\beta_{nc} = 0.71 \left(\frac{a_v d_p}{\epsilon} \right)^{0.65} \left(\frac{\rho_L^2 g d_p^3}{\mu_L^2} \right)^{-0.42} \left(\frac{\rho_L U_L d_p}{\mu_L} \right)^{0.53} \left(\frac{\rho_G U_G d_p}{\mu_G} \right)^{-0.31} \quad (13)$			
Ellman et al. (1990)	trickle bed	0.1–8.0	empirical
$\log \beta_{nc} = -R X_G^m Re_L^n We_L^p \left(\frac{a_v d_K}{1 - \epsilon} \right)^q \quad (14)$ <p>high interaction regime $R = 0.16; m = 0.325; n = 0.163; p = -0.13; q = -0.163$ low interaction regime $R = 0.42; m = 0.24; n = 0.14; p = 0; q = -0.14$</p>			
van Gelder and Westertep (1990)	flooded bed	0.2–1.2	empirical
$\epsilon \beta_e = 0.354 + 0.143 U_L^{0.405} - 0.206 \left(\frac{U_G}{U_L} \right)^{0.125} \quad (15)$			
Ring and Missen (1991)	trickle bed	10	empirical
$\epsilon \beta_a = 15.6 U_L^{0.679} \quad (16)$			
Wammes et al. (1991a) trickling, no gas flow	trickle bed	0.3–6.0	empirical
$\beta_{nc} = 16.3 \left(\frac{\rho_L U_L d_p}{\mu_L} \right)^c \left(\frac{\rho_L^2 g d_p^3}{\mu_L^2} \right)^d$ $c = \begin{cases} 0.36 & \text{if } Re < 11 \\ 0.55 & \text{if } Re > 15 \end{cases} \quad d = \begin{cases} -0.39 & \text{if } Re < 11 \\ -0.42 & \text{if } Re > 15 \end{cases} \quad (17)$ <p>gas-liquid flow (Specchia and Baldi (1977) correlation)</p> $\beta_{nc} = 3.8 \left(\frac{\rho_L U_L d_p}{\mu_L} \right)^{0.55} \left(\frac{\rho_L^2 g d_p^3}{\mu_L^2} \left(1 + \frac{\Delta P}{\rho_L g Z} \right) \right)^{-0.42} \left(\frac{a_v d_p}{\epsilon} \right)^{0.65}$			
Larachi et al. (1991a)	trickle bed	0.2–8.1	empirical
$\log(1 - \beta_e) = - \frac{1.22 We_L^{0.15}}{Re_L^{0.20} X_G^{0.15}} \quad (18)$			
Larachi et al. (1991b)	trickle/flooded bed	0.2–8.1	empirical
$\beta_e = 1 + \frac{J_{df} - U_G}{U_G + U_L} \quad (19)$ <p>where $J_{df} = A U_G^b$ (a, b depend on the gas-liquid-solid system)</p>			
Lara-Marquez et al. (1992)	flooded bed	0.3–5.1	empirical
$\log(1 - \beta_e) = - \frac{0.93 We_L^{0.08}}{Re_L^{0.20} X_G^{0.15}} \quad (20)$			

Table 6 (Continued)

author	flow configuration	P (MPa)	approach
Holub et al. (1992, 1993), Al-Dahhan and Dudukovic (1994) ^a	trickle bed	0.31–5	phenomenological
$\Psi_L = \frac{\Delta P}{\rho_L g Z} + 1 = \left(\frac{\epsilon}{\epsilon_L} \right)^3 \left[\frac{E_1 \bar{R} e_L}{(1 - \epsilon) G a_L} + \frac{E_2 \bar{R} e_L^2}{(1 - \epsilon)^2 G a_L} \right]$ $\Psi_G = \frac{\Delta P}{\rho_G g Z} + 1 = \left(\frac{\epsilon}{\epsilon - \epsilon_L} \right)^3 \left[\frac{E_1 \bar{R} e_G}{(1 - \epsilon) G a_G} + \frac{E_2 \bar{R} e_G^2}{(1 - \epsilon)^2 G a_G} \right]$ $\Psi_L = 1 + \frac{\rho_G}{\rho_L} (\Psi_G - 1) \quad (21)$			
Tsamatsoulis and Papayannakos (1994)	trickle bed	5.0	empirical
$\epsilon \beta_e = a U_L^b \text{ where } (a, b) \text{ depend on boundary conditions} \quad (22)$			

^a E_1 and E_2 are Ergun constants that characterize the bed and are determined from single-phase flow measurements. The third equation is first solved for liquid holdup, and then the first or the second equation is solved for pressure drop.

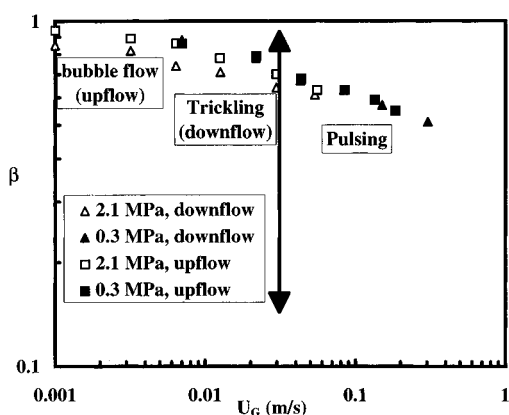


Figure 6. External ethylene glycol holdup as a function of superficial nitrogen velocity in bubble flow and pulse flow regimes in upflow (FBR) operation and trickle flow and pulse flow regimes in TBR operation. $P = 0.3, 2.1$ MPa (after Larachi, 1991).

in the trickling flow regime, the data were well described by the low interaction correlation of Specchia and Baldi (1977). For two-phase flow, their data were correlated using the modified high interaction correlation of Specchia and Baldi (1977).

Based on ENSIC's Nancy data bank of liquid holdups at atmospheric pressure, Ellman et al. (1990) derived two correlations for liquid holdup, one for the high and the other for the low interaction regimes. Good agreement was found between their high interaction regime correlation and water holdup under high-pressure nitrogen (up to 8.1 MPa) (Wild et al., 1991). Wammes et al. (1990a,b, 1991a,b) and Wammes and Westerterp (1990) investigated static and noncapillary liquid holdups by the stop-flow technique and bed drainage for the same operating conditions as used in the two-phase pressure drop studies. They reported that liquid holdup decreased when the pressure was increased for given gas and liquid superficial velocities for each of the three liquids tested (see Table 3). Such a decrease was interpreted as due to a shift in the reactor fluid dynamics from a state predominantly controlled by gravity (trickle flow with zero gas flow rate) to a state controlled by gas-liquid shear stress (or pressure drop). The Specchia and Baldi correlation (1977) for the low interaction regime described correctly their two-phase flow liquid holdup data. For trickling flow and zero gas flow (case 1 above of section 2) and $Re_L < 11$, liquid holdups were well described by available correlations

(Satterfield and Way, 1972; Goto and Smith, 1975), whereas for $Re_L > 15$, the Specchia and Baldi correlation (1977) for zero gas flow rate led to a good agreement.

Larachi et al. (1990, 1991a–d) and Wild et al. (1991) used the tracer impulse technique to investigate total liquid holdups within the same operating range as used in two-phase pressure drop measurements. The main conclusions drawn from their study are consistent with the discussion of section 2. They found that liquid holdup is insensitive to pressure for $U_G < 1–2$ cm/s, and the corresponding density rule was proposed for the estimation of liquid holdup in the presence of a light gas at high pressure knowing the holdup at atmospheric pressure in the presence of a heavy gas. A drift flux approach and a correlation were also developed for coalescing to weakly foaming systems (Table 6). Figure 6 shows some of Larachi et al.'s (1991a–d) liquid holdup data at high-pressure operation.

Ring and Missen (1991) investigated total, capillary, and dynamic liquid holdups during the catalytic hydrodesulfurization of dibenzothiophene in trickle flow at 10 MPa and 330–370 °C. The results showed the independence of liquid holdup upon temperature and pressure for the very low hydrogen mass fluxes tested ($53 \times 10^{-5} < G < 32 \times 10^{-4}$ kg/m²·s) and found that the available correlations derived for cold conditions (1 atm and 25 °C) can be useful for estimation purposes.

Al-Dahhan and Dudukovic (1994) measured liquid holdups using the stop-flow technique and bed drainage for the same conditions as for the pressure drops, i.e., trickle flow regime. They interpreted the evolution of liquid holdup as a function of gas density according to the five cases of their phenomenological analysis presented in section 2. By plotting liquid holdup as a function of superficial mass liquid velocity, they confirmed the observations made by Wammes et al. (1990a,b, 1991a,b), Wammes and Westerterp (1990, 1991), and Larachi et al. (1990, 1991a,b). Their high-pressure data were well described with the parameter-free phenomenological model of Holub et al. (Holub et al., 1992, 1993) and its extension (Al-Dahhan et al., 1996) (see Table 6). They found, within the operating conditions that they have studied, that Holub et al. (1992, 1993) mechanistic model and its extended version for high pressure predict liquid holdup and pressure drop better than the available high-pressure correlations.

Table 7. Correlations and Models for Prediction of Gas-Liquid Interfacial Areas in High-Pressure Trickle-Bed Reactors

author	flow configuration	P (MPa)	approach
Wild et al. (1992) low interaction	trickle bed	atmospheric and high pressure	empirical
$\frac{a}{a_v} = 10 \left[X_G Re_L^{-1/2} We_L \left(\frac{a_v d_K}{1 - \epsilon} \right)^{3/2} \right]^{0.7}$			
high interaction			
$\frac{a^\circ}{a_v} = 1550 \left[X_G Re_L^{-1/2} We_L \left(\frac{a_v d_K}{1 - \epsilon} \right)^{-5} \right]^{0.7}$			
transition regime			
$\frac{a}{a_v} = 21.3 \left[X_G Re_L^{-1/2} We_L \left(\frac{a_v d_K}{1 - \epsilon} \right)^{-2} \right]^{0.5} \quad (23)$			
Larachi (1991)	trickle bed	0.3–3.2	empirical
$\frac{a}{a_v} = 584 X_G^{0.86} Re_L^{1.48} Ka^{-0.5} \quad (24)$			
Cassanello et al. (1996)	trickle bed	0.3–3.2	phenomenological
$a = a^\circ \left\{ 1 + 4.9 \times 10^4 \left(\frac{\mu_G}{\mu_L} \right)^{1/6} \frac{We_L}{Re_L \epsilon} \left(1 + 2.5 \left(1 - \frac{\beta_e}{\beta_e^\circ} \right) \right) \left(\frac{1}{\beta_e} - \frac{1}{\beta_e^\circ} \right) \right\} \quad (25)$			

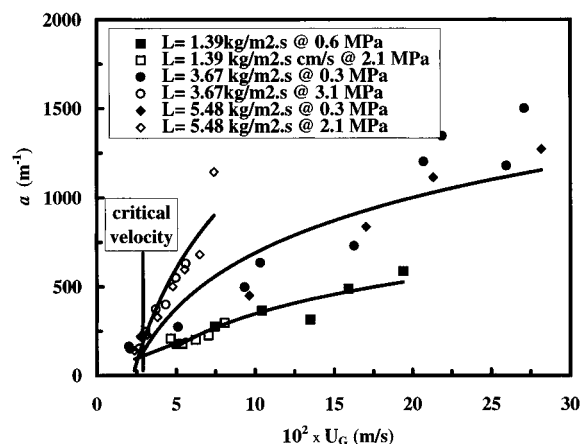


Figure 7. Effect of pressure and gas and liquid flow rates on gas-liquid interfacial areas in TBRs: system, 1.5 mol/L DEA (diethanolamine) in water/0.05 mole fraction CO_2 in a mixture of nitrogen and CO_2 ; equivalent particle diameter, 3.1 mm PVC extrudates; reactor diameter, 2.3 cm. Lines represent the trends (after Cassanello et al., 1996).

7. Gas-Liquid Mass-Transfer and Interfacial Area

In three-phase gas-liquid-solid systems such as TBRs, the gas-liquid mass-transfer resistance can have a detrimental effect on the overall reactor performance. Therefore, accurate estimation of the gas-liquid mass-transfer parameters is important for achieving successful reactor design or scaleup. In spite of the vast information found in the literature on gas-liquid mass-transfer characteristics of trickle beds at atmospheric pressure (Ellman, 1988), only a few researchers have studied how they evolve at elevated pressures (Larachi et al., 1992; Lara-Marquez et al., 1992; Wammes et al., 1991b; Wild et al., 1992). From these studies it was established that gas-liquid interfacial areas and volumetric mass-transfer coefficients are influenced by pressure in TBRs as shown in Figures 7 and 8, respectively. Table 3 shows the experimental ranges explored by these investigators, and Tables 7 and 8 list the models and correlations recently published on gas-liquid interfacial areas and liquid-side volumetric mass-

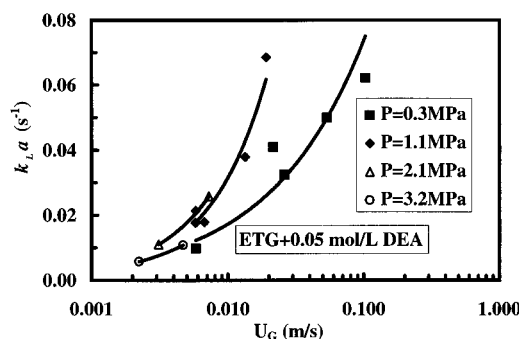


Figure 8. Effect of pressure (gas density) and gas flow rates on the volumetric gas-liquid mass-transfer coefficient at $L = 3.7$ kg/m²·s: system, ETG and 0.05 mol/L DEA/0.05 mole fraction CO_2 in a mixture of nitrogen and CO_2 ; particle diameter, 3.4 mm; reactor diameter, 2.3 cm. Lines represent the trend (after Lara-Marquez et al., 1992).

transfer coefficients. These parameters were determined in the trickling flow regime solely by the chemical method using CO_2 carbamation of diethanolamine aqueous or organic solutions. These studies report enhancement of gas-liquid mass-transfer with increasing pressures.

Based on the experimental study of interfacial areas and liquid-side volumetric mass-transfer coefficients at elevated pressure, the following observations can be made:

(a) Liquid-side volumetric mass-transfer coefficients and gas-liquid interfacial areas follow a trend qualitatively similar to pressure drops with regard to the mass fluxes or superficial velocities for a given pressure or gas density.

(b) For gas superficial velocity less than 1–2 cm/s, neither of the two mass-transfer parameters depends on gas density. There is still not enough information to assess the effect of pressure on the liquid-side mass-transfer coefficient k_L alone.

(c) For gas velocities larger than 1–2 cm/s and at a given liquid velocity, the gas-liquid interfacial area increases when pressure is increased. To interpret this effect, Cassanello et al. (1996) postulated that due to shear intensification the liquid trickling films are

Table 8. Correlations and Models for Prediction of Liquid-Side Gas-Liquid Volumetric Mass-Transfer Coefficient in High-Pressure Trickle-Bed Reactors

author	flow configuration	P (MPa)	approach
Wild et al. (1992) low interaction	trickle bed	atmospheric	empirical
			$\frac{k_L a^\circ d_K^2}{D_{AL}} = 2.8 \times 10^{-4} \left[X_G^{1/4} Re_L^{1/5} We_L^{1/5} Sc_L^{1/2} \left(\frac{a_v d_K}{1 - \epsilon} \right)^{1/4} \right]^{3.4}$
			high interaction
			$\frac{k_L a^\circ d_K^2}{D_{AL}} = 0.45 \left[X_G^{1/2} Re_L^{4/5} We_L^{1/5} Sc_L^{1/2} \left(\frac{a_v d_K}{1 - \epsilon} \right)^{1/4} \right]^{1.3}$
			transition regime
			$\frac{k_L a^\circ d_K^2}{D_{AL}} = 0.091 \left[X_G^{1/4} Re_L^{1/5} We_L^{1/5} Sc_L^{3/10} \left(\frac{a_v d_K}{1 - \epsilon} \right)^{1/4} \right]^{3.8} \quad (26)$
Cassanello et al. (1996)	trickle bed	0.3–3.2	phenomenological
			$k_L a = (k_L a)^\circ + k_L^{(Sh=2)} (a - a^\circ) \quad (27)$

Table 9. Correlations and Models for Prediction of Liquid-Solid Contacting Efficiency in High-Pressure Trickle-Bed Reactors

author	flow configuration	P (MPa)	approach
Ruecker and Akgerman (1987)	trickle bed	5.2	empirical
			$\eta_{CE} = 1 + 0.14\pi_{LV} - 1.17\pi_{LV}^2 \quad (28)$
Ring and Missen (1991)	trickle bed	10	empirical
			$\eta_{CE} = 1 - \exp(-644 U_L^{0.964})$ based on diffusivity ratio
			$\eta_{CE} = 1 - \exp(-118 U_L^{0.635})$ based on diffusivity square root ratio
Al-Dahhan and Dudukovic (1995)	trickle bed	0.31–5	semiempirical
			$\eta_{CE} = 1.104 (\overline{Re})^{1/3} \left[\frac{\frac{\Delta P}{\rho_L g Z} + 1}{Ga_L} \right]^{1/9} \quad (30)$

invaded by tiny bubbles whose size results from a balance between viscosity and surface tension forces. It is the formation of such small bubbles that enhances the interfacial area and the volumetric mass-transfer coefficient. A simple model was then derived in which the interfacial area at high pressure is split into two contributions, that of liquid spreading on the solids and that due to transported gas bubbles which give rise to the pressure dependence of the gas-liquid mass-transfer. This model is given in Tables 7 and 8. According to the phenomenological analysis for the effects of pressure proposed by Al-Dahhan and Dudukovic (1994, 1995), the liquid film thickness at a fixed liquid mass velocity decreases with pressure and gas velocity where the shear stress on the gas-liquid interface increases. This results in an improved spreading of the liquid film over the external packing area, making them more wet and at the same time increasing the gas-liquid interfacial area.

8. Catalyst Wetting Efficiency

External catalyst wetting efficiency is an important design and scale-up parameter in determining the degree of catalyst utilization in trickle-bed reactors (the internal contacting is usually equal to unity due to capillary effects). The available predictions of wetting efficiency rest on data collected at atmospheric pressure (Shulman et al., 1955; Onda et al., 1967; Krauze and Serwinski, 1971; Puranik and Vogelpohl, 1974; Mills and Dudukovic, 1981; El-Hisnawi, 1981; El-Hisnawi et al., 1981; Lazzaroni et al., 1988). Although Ring and

Missen (1991) and Ruecker and Akgerman (1987) measured the contacting efficiency at 10 and 5.2 MPa, they did not investigate the effect of high pressure. Table 9 lists the wetting efficiency correlations developed for the high pressure/temperature laboratory-scale trickle-beds. Al-Dahhan and Dudukovic (1995) have studied the catalyst wetting efficiency at high-pressure operation via a tracer technique (see Table 3). In their work, a phenomenological analysis was developed to relate the wetting efficiency with operating conditions such as reactor pressure and gas and liquid flow rate which resulted in the five limiting cases as shown in Figure 2c. For a fixed liquid mass velocity, at high pressure and high gas flow rates, wetting efficiency improves noticeably whereas pressure drop increases significantly and liquid holdup decreases considerably. As liquid flow rate increases, contacting efficiency improves further due to an increase in both pressure drop and liquid holdup. The effect of gas flow rate on the wetting efficiency, pressure drop, and liquid holdup is more pronounced at elevated pressure (see Figure 2a-c). The improvement in wetting efficiency with increased gas flow rate is due to the improved spreading of the liquid holdup over the external packing area. This is supported by the finding of Larachi et al. (1992) where the gas-liquid interfacial area increases at high pressure and high gas flow rate operation. Al-Dahhan and Dudukovic (1995) developed a correlation for wetting efficiency for high-pressure operation given by eq 30 of Table 9. This correlation is also in good agreement with the atmospheric data collected previously and provides the means for assessing liquid-catalyst contacting at high operating pressures.

9. Catalyst Dilution with Inert Fines in Laboratory-Scale TBRs

Since laboratory-scale reactors need to match the space velocity of commercial units, the actual velocities in them are much lower, which leads to incomplete catalyst wetting. Moreover, the same catalyst sizes, types, and shapes employed in the commercial reactors are used in the small-diameter laboratory units where the criterion $D_c/d_p > 20$, desirable for avoiding wall effects, usually cannot be met. Such conditions can cause liquid maldistribution and insufficient use of the catalyst bed for liquid-limited reactions by reducing liquid-solid contacting efficiency (Al-Dahhan and Dudukovic, 1995; Wu et al., 1996a; Sie, 1991; Van Klinken and Van Dongen, 1980; Gierman, 1988). As a remedy to the above problems, dilution of the laboratory beds with fines (small, inert, and nonporous particles of about 0.1 catalyst diameter) has been recommended and utilized for decades to overcome the shortcomings of laboratory-scale reactors and/or to provide better temperature uniformity in the reactor particularly for highly exothermic reactions. In this technique, the hydrodynamics is largely dictated by the packing of fines, whereas the catalytic phenomena are governed by the catalyst particle of the same shape, size, and form as used in the commercial reactors. It is noteworthy that the utility of the dilution techniques would be negated if the packing method of mixing the bed of catalyst and fines failed to produce reproducible results. Al-Dahhan et al. (1995) developed a reproducible procedure for packing small-diameter packed beds with a mixture of fines and catalyst which relies on filling the original bed voids with fines; the step-by-step procedure is reported in Al-Dahhan et al. (1995) and Al-Dahhan and Dudukovic (1996). Al-Dahhan and Dudukovic (1996) also measured the liquid-catalyst contacting efficiency in a diluted bed, with fines and compared it to that obtained in a nondiluted bed, both beds being operated under high pressure at the same set of liquid mass velocity. They reported that fines improve catalyst wetting efficiency, which in a diluted bed is strongly related to both pressure drop and liquid holdup as shown in Figure 9a–c. Thus, in a diluted bed, while wetting efficiency improves at high pressure and high gas flow rates, pressure drop increases and liquid holdup decreases.

10. Liquid-Limited and Gas-Limited Reactions in High-Pressure TBRs

Wu et al. (1996a,b) and Khadilkar et al. (1996) studied the effect of catalyst wetting at high pressure on the performance of TBRs. Comparisons have been made between the performance of trickle flow (partially wetted catalyst) and upflow, flooded-bed reactor (FBR; completely wetted catalyst) without fines and for both TBR and FBR with fines (completely wetted catalyst in each reactor). Hydrogenation of α -methylstyrene (in hexane solvent) to cumene over 2.5% alumina-supported palladium catalyst extrudates was used as a test reaction ($A(g) + bB(l, \text{nonvolatile}) \rightarrow \text{product}(l)$) (Wu et al., 1996a). A simple and usable criterion for identifying gas or liquid limitation has been suggested based on the relative availability of the reactant species at the reaction site. For the hydrogenation of α -methylstyrene (α -MS), a value of $D_{eB}C_{Bi}/b(D_{eA}C_A^*) \gg 1$ would imply gaseous reactant limitation, while $D_{eB}C_{Bi}/b(D_{eA}C_A^*) \ll 1$ indicates liquid reactant limitation (Wu et al., 1996a). Hence, this reaction was found to be gas-limited at low

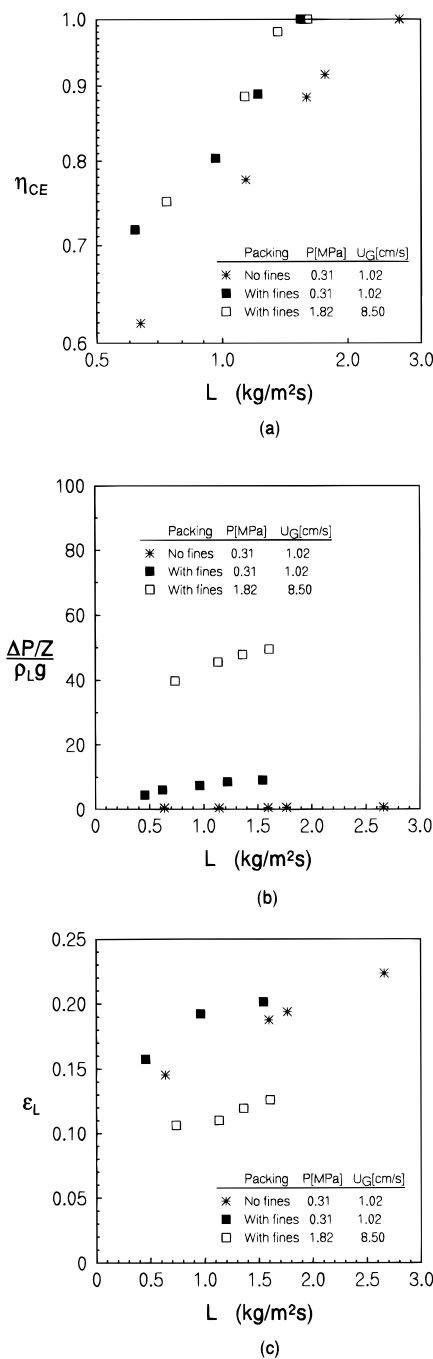


Figure 9. Effect of fines on catalyst wetting efficiency (a), pressure drop (b), and liquid holdup (c) in a diluted bed of extrudates: vol. fines/vol. cat. = 0.54; particle size, 0.157×0.43 cm; fines, 0.2 mm silicon carbide; reactor diameter, 2.2 cm (packed according to Al-Dahhan et al. (1995) procedure) (after Al-Dahhan and Dudukovic, 1996).

pressure and high feed concentrations of α -MS but became liquid-limited at high pressure (>200 psig) and low α -MS feed concentrations. Also it was found (Wu et al., 1996a) that a TBR performs better than the upflow reactor (FBR) with fully wetted catalyst at low pressures and high feed concentrations of α -MS when the reaction is gas limited, due to ready access of the gas to the incompletely wetted external catalyst area. In contrast the upflow reactor (FBR) performs better at high pressure when liquid reactant limitation controls the rate, due to the completely wetted catalyst in the upflow reactor. Since low molecular weight gas (hydrogen) is used, the effect of pressure and gas velocity employed in their study on the catalyst wetting

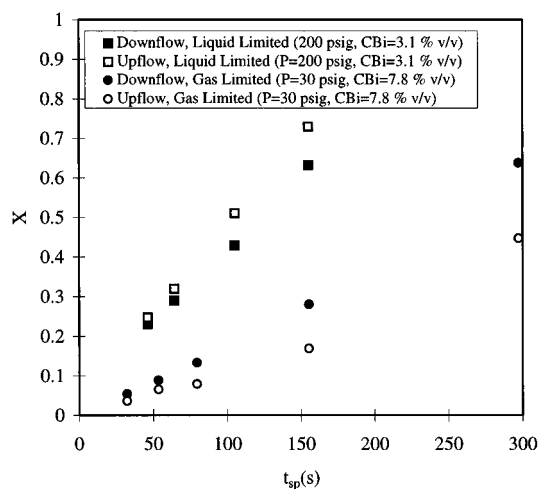


Figure 10. Comparison between trickle-bed and upflow performance at actual gas velocity = 4.4 cm/s. X : conversion. t_{sp} : space time (s) (3600/LHSV). (a) Gas-limited reaction; (b) liquid-limited reaction. System: hydrogenation of α -methylstyrene (in hexane solvent) to cumene over 2.5% alumina-supported palladium catalyst extrudates. Particle size: 0.13×0.56 cm. Reactor diameter: 2.2 cm (after Wu et al., 1996a).

efficiency in TBR is insignificant. As liquid mass velocity is increased (i.e., space time is decreased), the performance of TBR approaches that of FBR due to the increase in the wetting efficiency of TBR toward complete wetting. Figure 10 illustrates the performance comparison of TBR and FBR without inert fines. The conversions are higher in both TBR (downflow) and FBR (upflow) reactors operated under liquid-limited reaction than those obtained in these reactors operated under gas-limited reactions. The effects of reactor pressure, liquid reactant feed concentration, and gas velocity on the performance of these reactors for both gas- and liquid-limited conditions that explain such observations are discussed in detail by Wu et al. (1996a). However, the performance of both downflow and upflow improves with the reactor pressure due to an increase in the gas solubility which helps the rate of transport to the wetted catalyst (in both modes) and improves the driving force for gas to catalyst mass-transfer to the inactive wetted catalyst in the downflow mode. At low feed concentration of the liquid reactant (α -methylstyrene (C_{Bi}) = 3.1% v/v) and high pressure (> 100 psig), the reaction becomes liquid reactant limited, where no further enhancement is observed when pressure is increased from 100 to 200 psig (where the ratio $D_{eB}C_{Bi}/b(D_{eA}C_A^*)$ drops from 1.5 at 100 psig to 0.8 at 200 psig). This means that any further increase in the reactor pressure, and hence liquid phase hydrogen concentration, will have a minimal effect since hydrogen is not the limiting reactant anymore (i.e., the effect of pressure diminishes when liquid limitation is approached). Moreover, when liquid limitation is observed, there is no effect of liquid reactant feed concentration (C_{Bi}) on its conversion in either mode of operation. This is a result of the liquid reactant transport or intrinsic rate limitation which shows up as a first-order dependence, making conversion independent of feed concentration. At high initial liquid reactant feed concentration (C_{Bi} = 7.8% v/v) and low pressure (30 psig) (relatively close to the atmospheric pressure), the hydrogenation of α -methylstyrene becomes gas limited and is known to exhibit a zeroth-order behavior with respect to α -methylstyrene and first order with respect to hydrogen (Beaudry et al., 1986; Wu et al., 1996a,b). Hence, an inverse proportionality

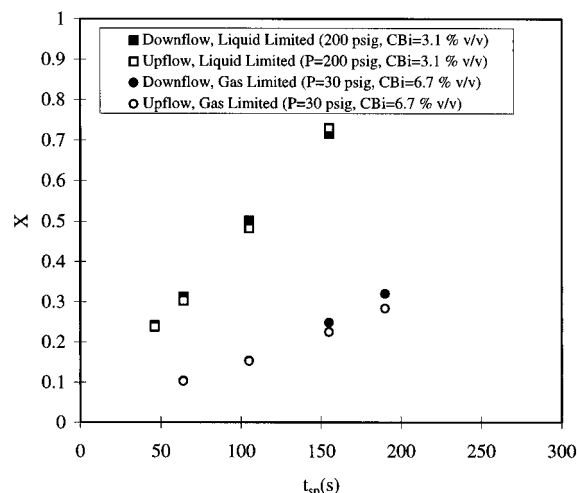


Figure 11. Effect of inert fines on the performance of trickle-bed and upflow reactors at actual gas velocity = 4.4 cm/s. X : conversion. t_{sp} : space time (s) (3600/LHSV). (a) Gas-limited reaction; (b) liquid-limited reaction. System: hydrogenation of α -methylstyrene (in hexane solvent) to cumene over 2.5% alumina-supported palladium catalyst extrudates. Particle size: 0.13×0.56 cm. Fines: 0.2 mm silicon carbide. Reactor diameter: 2.2 cm (after Wu et al., 1996a).

of conversion with liquid reactant feed concentration (typical of zero-order behavior) was observed. The effect of gas velocity on the reactor performance for both modes of operation (i.e., TBR and FBR) at all the feed concentrations tested was found to be insignificant in the range of hydrogen velocities (3.8–14.4 cm/s) and reactor pressures (30–300 psig) studied (Wu et al., 1996a; Khadilkar et al., 1996).

In beds diluted with fines, it was found that both trickle bed and upflow perform identically under both gas- and liquid-limited conditions as shown in Figure 11, corroborating the fact that the fluid dynamics and kinetics can be decoupled by using fines. This implies that the performance of the diluted bed is not dependent on the reactant limitation and flow mode used. This conclusion is important in establishing the use of fines in laboratory-scale reactors as an effective and viable scale-up tool possibly to be preferred to upflow reactors. Indeed, in the later case, complete wetting occurs at the expense of increased liquid holdup, which in return can alter the relative extent of homogeneous and heterogeneous reactions occurring in more complex systems and should therefore be avoided. In contrast, in the bed packed with fines, wetting is increased without a significant increase in liquid holdup. Wu et al.'s (1996a) study also demonstrated that the advantage of upflow or downflow depends on whether liquid or gas reactant is rate-limiting and that a single criterion proposed for identifying the limiting reactant can explain most of the data reported in the literature on these two modes of operation.

11. Evaluation of TBR Models

Most of the reported investigations in the literature have suggested a plug flow model for the liquid phase modified by consideration of some other factors such as external liquid holdup, external contacting, catalyst effectiveness, etc. Wu et al. (1996b) have evaluated the current plug flow models (Dudukovic, 1977; Henry and Gilbert, 1973; Mears, 1974) for first-order reactions in high-pressure TBRs using the isothermal decomposition of hydrogen peroxide on a Cu–Cr catalyst as shown in Figure 12. Comparison of model predictions and ex-

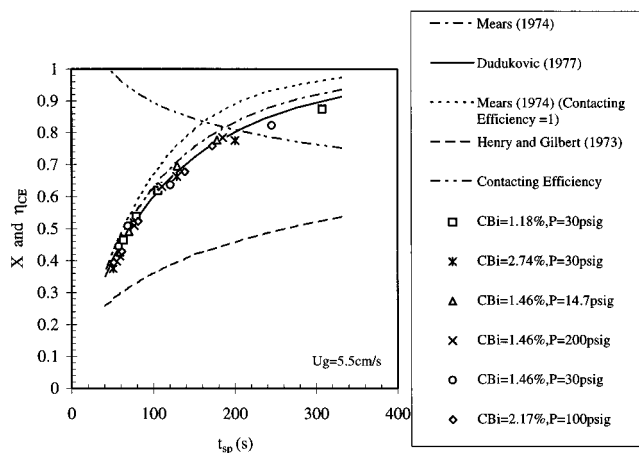


Figure 12. Comparison of model predictions and experimental data for trickle-bed reactors. X : conversion. t_{sp} : space time (s) (3600/LHSV). η_{CE} : catalyst wetting efficiency. System: liquid phase decomposition of hydrogen peroxide in water (first order reaction). Particles: copper chromite $1/16$ in. extrudates. Reactor diameter: 2.2 cm (after Wu et al., 1996b).

perimental data indicates that both external mass-transfer effects and incomplete external catalyst wetting need to be accounted for. Dudukovic (1977) and Beaudry et al. (1987) pellet-scale approximate models for the catalyst effectiveness factor adequately simulate both effects (Wu et al., 1996b). Khadilkar et al. (1996) evaluated the performance prediction for both TBR and upflow reactors at high pressure using the reactor-scale model of El-Hisnawi et al. (1981) and pellet-scale models (Beaudry et al., 1987; Harold and Watson, 1993). Both gas- and liquid-limited reactions were used for such an evaluation. Hydrogenation of α -methylstyrene in hexane to cumene over 2.5% Pd alumina catalyst particles was used as a test reaction for both the gas-limited case, at low pressure and high feed α -MS concentration, and the liquid-limited case, at high pressure and low feed α -MS concentration as mentioned above (Wu et al., 1996a). They found, as shown in Figure 13a,b, that the predictions of the reactor-scale and pellet-scale models are satisfactory for the current conditions. These predictions could be improved by using reliable high-pressure correlations for mass-transfer coefficient and interfacial area, especially in cases where the rate is significantly affected by external mass transfer.

12. Concluding Remarks

Based on our review of the available recent investigations conducted in high-pressure TBRs, the effect of pressure on the design and scale-up parameters, such as flow regime transition, pressure drop, liquid holdup, catalyst wetting efficiency, and gas-liquid interfacial area and mass-transfer, can be described based on the five limiting cases proposed by Al-Dahhan and Dudukovic (1994, 1995) discussed in section 2. The effect of pressure arises due to an increase in gas density and, hence, can be simulated by the increase in molecular weight of the gas. When the pressures of gases of different molecular weight are set in such a manner so as to provide equal gas densities, the effects on the TBR fluid dynamics are about the same.

If the superficial gas velocity is below 2 cm/s (cases 2 and 4, section 2), pressure (or gas density) effects are minimal so that a pressurized TBR behaves as if operated at about 1 atm. For the operating conditions in which gas has sufficient inertia, $\rho_G U_G^2 \geq 1\% \rho_L U_L^2$,

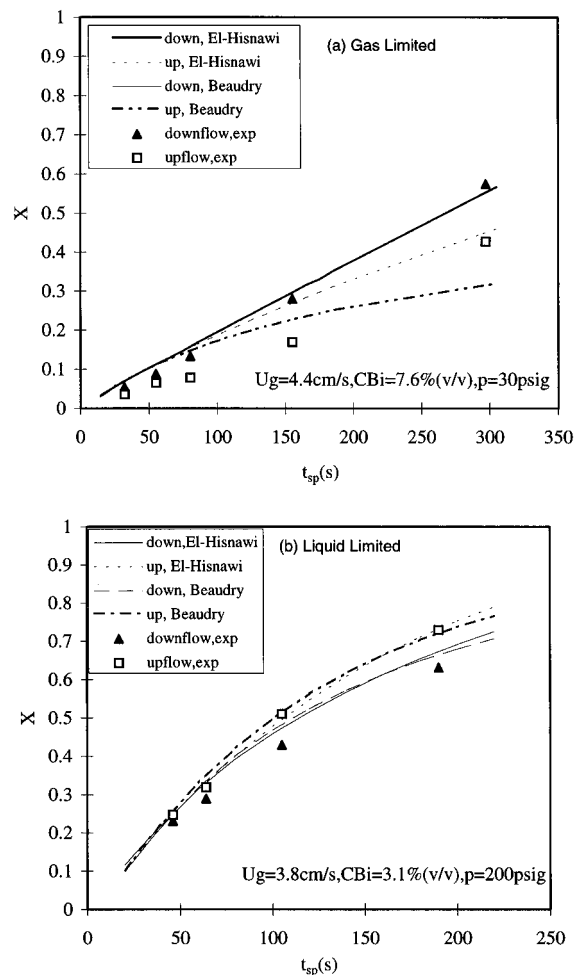


Figure 13. Comparison between model predictions and experimental data for the performance of trickle-bed and upflow reactors: (a) gas limited reaction; (b) liquid limited reactions. X : conversion. t_{sp} : space time (s) (3600/LHSV). System: hydrogenation of α -methylstyrene (in hexane solvent) to cumene over 2.5% alumina-supported palladium catalyst extrudates. Particle size: 0.13×0.56 cm. Fines: 0.2 mm silicon carbide. Reactor diameter: 2.2 cm (after Khadilkar et al., 1996).

the pressure drop at high-pressure operation is equal to the pressure drop at atmospheric pressure. However, at high pressure and high gas flow rate (case 5, section 2), the pressure drop increases considerably, liquid holdup decreases significantly, catalyst wetting efficiency improves, gas-liquid interfacial area and volumetric mass-transfer coefficient increase, and the trickle-to-pulse transition shifts toward higher liquid flow rates (i.e., the trickle flow regime becomes wider at elevated pressure). At liquid velocities corresponding to the dispersed bubble flow regime, higher gas velocities are required to bring pulse flow.

The improvement in catalyst wetting efficiency due to diluting the bed with fines is enhanced further at high pressure and high gas flow rate, which result in higher pressure drop and lower liquid holdup.

Trickle-bed reactor (TBR) outperforms the upflow reactor (FBR) for gas-limited reaction, while the latter performs better than TBR for a liquid-limited reaction. The performance of these reactors becomes similar only at high liquid mass velocities and/or high pressure and high gas velocity when the catalyst in TBR becomes completely wetted similar to that usually encountered in the upflow reactor (FBR). However, in a diluted bed with fines both the trickle-bed and upflow reactor perform identically under both gas- and liquid-limited

conditions, confirming the fact that the fluid dynamics and kinetics can be decoupled by using fines. The performance predictions of the current trickle-bed reactor models for the investigations presented in the review are satisfactory for both gas- and liquid-limited reactions.

It is evident that atmospheric data and models or correlations cannot, in general, be extrapolated to operation at elevated pressures particularly conditions of high gas flow rate and high gas molecular weight. This can only be accomplished in some special cases mentioned in this paper.

It is noteworthy to mention that it is valuable to compare the high-pressure laboratory data and the correlations prediction with large-scale trickle-bed reactor data to demonstrate the applicability of the high-pressure findings and correlations and models for scaleup or scaledown. Unfortunately, this is not included in this paper due to the unavailability of the high-pressure large-scale industrial trickle-bed reactor data for the parameters discussed in this paper.

Clearly, a lot of work remains to be done in providing a fundamentally based description of the effect of pressure on the parameters of importance in TBR operation, design, and scaleup or scaledown.

Nomenclature

a = gas-liquid interfacial area, m^2/m^3

a_v = bed-specific surface area, m^2/m^3

C^* = gas solubility

C_A^* = concentration of gaseous reactant in the liquid phase, mol/m^3

C_{Bi} = concentration of liquid reactant in liquid, mol/m^3

C_p = heat capacity at constant pressure, $kcal/kg/K$

D = molecular diffusivity, m^2/s or cm^2/s

D_{eA} = effective diffusivity of gaseous reactant in the catalyst, m^2/s

D_{eB} = effective diffusivity of liquid reactant in the catalyst, m^2/s

D_c = column diameter, m

D_z = axial dispersion coefficient, m^2/s

d_K = Krischer-Kast hydraulic diameter, m

$$d_p \sqrt[3]{\frac{16\epsilon^3}{9\pi(1-\epsilon)^2}}$$

d_p = particle diameter, m

E_1, E_2 = Ergun constants, eq 21

f = two-phase flow friction factor,

$$\frac{\Delta P/Z d_K}{2\rho_G U_G^2}$$

F_i = volume-averaged forces exerted on phase i by the other phases, N/m^3

Fr = Froude number, U^2/gd_p

G = gas mass flux, $kg/m^2 \cdot s$

g = gravitational acceleration, m/s^2

Ga = Galileo number,

$$\frac{d_p^3 \rho^2 g \epsilon^3}{\mu^2 (1-\epsilon)^3}$$

H = Henry's constant

J_{df} = drift flux, m/s

Ka = Kapitza dimensionless number,

$$\frac{\sigma_L^3 \rho_L}{\mu_L^4 g}$$

$k_L a$ = volumetric liquid-side mass-transfer coefficient, s^{-1}

L = liquid mass flux, $kg/m^2 \cdot s$

LHSV = liquid hourly space velocity (superficial velocity/bed length), $1/s$

P = pressure, MPa

Q = volumetric flow rate, mL/s

Re = Reynolds number, $\rho U d_p / \mu$

\overline{Re} = Reynolds number (modified),

$$\frac{\rho U d_p}{\mu(1-\epsilon)}$$

S = selectivity

Sc = Schmidt number, $\mu/\rho D$

T = temperature, K

t = time, s

t_{sp} = space time ($3600/LHSV$), s

U = superficial velocity, m/s

V = interstitial velocity, m/s

We_L = liquid Weber number,

$$\frac{\rho_L U_L^2 d_p}{\sigma_L}$$

X = conversion

X_G = modified Lockhart-Martinelli ratio,

$$\frac{U_G \sqrt{\rho_G}}{U_L \sqrt{\rho_L}}$$

Z = bed length, cm

Greek Letters

α_t = bed-to-wall heat transfer coefficient, $W/m^2 \cdot K$

β = liquid saturation

$\Delta P/Z$ = pressure drop

ϵ = bed porosity

ϵ_L = liquid holdup

Φ = density correction in Charpentier diagram, see eq 2

η_{CE} = wetting efficiency

κ = thermal conductivity, $J/m \cdot s \cdot K$

λ = dimensionless parameter in eq 2,

$$\sqrt{\frac{\rho_G \rho_L}{\rho_a \rho_w}}$$

μ = dynamic viscosity, $Pa \cdot s$

π_{LV} = vapor-to-feed molar ratio

ρ = density, kg/m^3

σ = surface tension, N/m

τ_{LG} = gas-liquid interfacial shear stress, Pa

ψ = dimensionless parameter in eq 2,

$$\frac{\sigma_w (\mu_L)^{1/3} (\rho_w)^{2/3}}{\sigma_L (\mu_w) (\rho_L)}$$

Subscripts

AL = gaseous reactant dissolved in liquid

a = active liquid holdup, or air

e = external liquid holdup

G = gas

GL = two-phase

L = liquid
 mix = mixture
 nc = noncapillary
 r = reduced
 trans = transition
 w = water

Superscript

° = atmospheric

Acronyms

DBT = dibenzothiophene
 DEA = diethanolamine
 ETG = ethylene glycol
 FBR = flooded-bed reactor
 HIR = high interaction regime
 HVGO = heavy gas oil
 LIR = low interaction regime
 PC = propylene carbonate
 TBR = trickle-bed reactor
 ↓ = downflow
 ↑ = upflow

Literature Cited

- Abbott, M. D.; Moore, G. R.; Ralph, J. L. Proceedings of the 7th ABG Conference. In *Gas-liquid-solid reactor design*; Shah, Y. T., Ed.; McGraw-Hill: New York, 1979; Paper S-4.
- Al-Dahhan, M. H. Effects of High Pressure and Fines on the Hydrodynamics of Trickle-Bed Reactors. D.Sc. Dissertation, Washington University, St. Louis, MO, 1993.
- Al-Dahhan, M. H.; Dudukovic, M. P. Pressure Drop and Liquid Hold-up in High Pressure Trickle-Bed Reactors. *Chem. Eng. Sci.* **1994**, *49*, 5681.
- Al-Dahhan, M. H.; Dudukovic, M. P. Catalyst Wetting Efficiency in Trickle-Bed Reactors at High Pressure. *Chem. Eng. Sci.* **1995**, *50*, 2377.
- Al-Dahhan, M. H.; Dudukovic, M. P. Catalyst Bed Dilution for Improving Catalyst Wetting in Laboratory Trickle-Bed Reactors. *AIChE J.* **1996**, *42*, 2594.
- Al-Dahhan, M. H.; Wu, Y. X.; Dudukovic, M. P. Reproducible Technique for Packing Laboratory-Scale Trickle-Bed Reactors with a Mixture of Catalyst and Fines. *Ind. Eng. Chem. Res.* **1995**, *34*, 741.
- Al-Dahhan, M. H.; Wu, Y. X.; Khadilkar, M. R.; Dudukovic, M. P. Improved Prediction of Pressure Drop and Liquid Hold-up in High Pressure Trickle-Bed Reactors. *5th World Congress of Chemical Engineering*; Symposium 3: Advanced Fundamentals, Session: Catalysis, Kinetics and Reaction Engineering, San Diego, CA, July 14–18, 1996, American Institute of Chemical Engineering (AIChE): New York, 1996; Vol. 1, p 209.
- Babu, S. P.; Shah, B.; Talwalkar, A. Fluidization Correlations for Coal Gasification Materials—Minimum Fluidization Velocity and Fluidized Bed Expansion Ratio. *AIChE Symp. Ser.* **1978**, *74*, 176.
- Bailey, J. E.; Ollis, D. F. *Biochemical Engineering Fundamentals*, 2nd ed.; McGraw-Hill Book Co. New York, 1986.
- Baker, B., III. Determination of the Extent of Catalyst Utilization in a Trickle-Flow Reactor. *ACS Symp. Ser.* **1978**, *65*, 425.
- Baldi, G. Design and Scale-up of Trickle-Bed Reactors. Solid-Liquid Contacting Effectiveness. In *Multiphase Chemical Reactors*; Rodrigues, A. E., Calo, J. M., Sweed, N. H., Eds.; NATO Advanced Study Institute Series E; Sitjhoff & Noordhoff: Aalphen aan den Rijn, The Netherlands, 1981a; Vol. 52, p 323.
- Baldi, G. Heat Transfer in Gas-Liquid-Solid Reactors. In *Multiphase Chemical Reactors*; Rodrigues, A. E., Calo, J. M., Sweed, N. H., Eds.; NATO Advanced Study Institute Series E; Sitjhoff & Noordhoff: Aalphen aan den Rijn, The Netherlands, 1981b; Vol. 52, p 307.
- Baldi, G. Hydrodynamics of Multiphase Reactors. In *Multiphase Chemical Reactors*; Rodrigues, A. E., Calo, J. M., Sweed, N. H., Eds.; NATO Adv. Study Inst. Series E, Sitjhoff & Noordhoff: Aalphen aan den Rijn, The Netherlands, 1981c; Vol. 52, p 271.
- Baldi, G.; Gianetto, A.; Sicardi, S.; Specchia, V.; Mazzarino, I. Oxidation of Ethyl Alcohol in Trickle-Bed Reactors: Analysis of the Conversion Rate. *Can. J. Chem. Eng.* **1985**, *63*, 62.
- Beaudry, E. G.; Mills, P. L.; Dudukovic, M. P. Gas-Liquid Downflow, Upflow, and Countercurrent Flow in Packed Beds—Reactor Performance for Gas Limiting Reaction. World Congress III of Chemical Engineering, Tokyo, Japan, Sept 1986; Paper 9b-152, p IV-173.
- Beaudry, E. G.; Dudukovic, M. P.; Mills, P. L. Trickle-Bed Reactors: Liquid Diffusional Effects in a Gas-Limited Reaction. *AIChE J.* **1987**, *33*, 1435.
- Belhaj, M. S. Design, Analysis and Modeling of an Enzymatic Oxidation Three-Phase Reactor Using Immobilized Enzymes (Conception, Analyse et Modélisation d'un Réacteur d'Oxydation Enzymatique Triphase à Enzymes Immobilisées). Ph.D. Dissertation, Université de Technologie de Compiègne, Compiègne, France, 1984.
- Cassanello, M.; Larachi, F.; Laurent, A.; Wild, G.; Midoux, N. Gas-Liquid Mass Transfer in High Pressure Trickle-Bed Reactors: Experiments and Modeling. In 3rd International Symposium on High Pressure Chemical Engineering, Zürich, Switzerland, Oct 7–9, 1996; Rudolf von Rohr, Ph., Trepp, Ch., Eds.; High Pressure Chemical Engineering; Amsterdam Process Technology Proceedings; Elsevier: Amsterdam, The Netherlands, 1996; Vol. 12, p 493.
- Charpentier, J. C. Recent Progress in Two-Phase Gas-Liquid Mass Transfer in Packed Beds. *Chem. Eng. J.* **1976**, *11*, 161.
- Charpentier, J. C. Gas-Liquid Reactors. In *Chemical Reaction Engineering Reviews*; Luss, D., Weekman, V. W., Eds.; ACS Symposium Series 72; American Chemical Society: Washington, DC, 1978; p 223.
- Charpentier, J. C. Hydrodynamics of Two-Phase Flow Through Porous Media. In *Chemical Engineering of Gas-Liquid-Solid Catalyst Reactions*; L'Homme, G. A., Ed.; CEBEDOC: Liège, Belgium, 1979; p. 78.
- Charpentier, J. C. What's New in Absorption with Chemical Reaction. *Trans. Inst. Chem. Eng.* **1982**, *60*, 131.
- Charpentier, J. C. Mass Transfer in Fixed Bed Reactors. In *Multiphase Chemical Reactors—Theory, Design, Scale-up*; Gianetto, A., Silveston, P. L., Eds.; Hemisphere Publ. Co.: Washington, 1986; p 289.
- Charpentier, J. C.; Favier, M. Some Liquid Hold-up Experimental Data in Trickle-Bed Reactors for Foaming and Nonfoaming Hydrocarbons. *AIChE J.* **1975**, *21*, 1213.
- Charpentier, J. C.; Bakos, M.; LeGoff, P. Question IV, Rapport 10, Société Hydrotechnique de France, *XII emes Journées de l'Hydraulique*, Paris, 1972.
- Chen, S.; Chuang, K. T. Simultaneous Methanol Removal and Destruction from Wastewater in a Trickle-Bed Reactor. *Can. J. Chem. Eng.* **1992**, *70*, 727.
- Crine, M.; L'Homme, G. Recent Trends in the Modelling of Catalytic Trickle-Bed Reactors. In *Mass Transfer with Chemical Reaction in Multiphase Systems: Three-Phase Systems*; Alper, E., Ed.; Martinus Nijhoff Publ.: The Hague, The Netherlands, 1983; Vol. II; p 99.
- Dankworth, D. C.; Sundaresan, S. Time-Dependent Vertical Gas-Liquid Flow in Packed Beds. *Chem. Eng. Sci.* **1992**, *47*, 337.
- Dankworth, D. C.; Kevrekidis, I. G.; Sundaresan, S. Dynamics of Pulsing Flow in Trickle Beds. *AIChE J.* **1990a**, *36*, 605.
- Dankworth, D. C.; Kevrekidis, I. G.; Sundaresan, S. Time-Dependent Hydrodynamics in Multiphase Flow. *Chem. Eng. Sci.* **1990b**, *45*, 2239.
- Diks, R. M.; Ottengraf, S. P. P. Verification of a Simplified Model for Removal of Dichloromethane from Waste Gases Using a Biological Tricking Filter. *Bioprocess Eng.* **1991**, *6*, 131.
- Dimenstein, D. M.; Ng, K. M. A Model for Pulsing Flow in Cocurrent Downflow Trickle Bed Reactors. *Chem. Eng. Commun.* **1986**, *41*, 215.
- Dimenstein, D. M.; Zimmerman, S. P.; Ng, K. M. Tricking and Pulsing Transition in Cocurrent Downflow Trickle-Bed Reactors with Special Reference to Large-Scale Columns. *ACS Symp. Ser.* **1984**, *234*, 3.
- Dirkx, J. M. H. De Trickle-Bed Reactor Part I. *Polytech. Tijdschr.: Procestech.* **1979a**, *34*, 227.
- Dirkx, J. M. H. De Trickle-Bed Reactor Part II. *Polytech. Tijdschr.: Procestech.* **1979b**, *34*, 316.
- Dudukovic, M. P. Catalyst Effectiveness Factor and Contacting Efficiency in Trickle-Bed Reactors. *AIChE J.* **1977**, *23*, 940.
- Dudukovic, M. P.; Mills, P. L. Catalyst Effectiveness Factors in Trickle-Bed Reactors. *ACS Symp. Ser.* **1978**, *65*, 387.
- Dudukovic, M. P.; Mills, P. L. Contacting and Hydrodynamics in Trickle-Bed Reactors. In *Encyclopedia of Fluid Mechanics*:

- Gas-Liquid Flows*; Cheremisinoff, N. P., Eds.; Gulf Publ. Corp.: Houston, TX, 1986; Vol. 3, p 969.
- Dudukovic, M. P.; Devanathan, N.; Holub, R. Multiphase Reactors: Models and Experimental Verification. *Rev. Inst. Fr. Pet.* **1991**, *46*, 439.
- Dwivedi, P. N.; Upadhyay, S. N. Particle-Fluid Mass Transfer in Fixed and Fluidized Beds. *Ind. Eng. Chem. Process Des. Dev.* **1977**, *16*, 157.
- El-Hisnawi, A. A. Tracer and Reaction Studies in Trickle-Bed Reactors. D.Sc. Dissertation, Washington University, St. Louis, MO, 1981.
- El-Hisnawi, A. A.; Dudukovic, M. P.; Mills, P. L. Trickle-Bed Reactors: Dynamic Tracer Tests, Reaction Studies and Modeling of Reactor Performance. *ACS Symp. Ser.* **1981**, *196*, 421.
- Ellman, M. J. Characteristics of CoCurrent Downflow Three-Phase Fixed-Bed Reactors (Caractéristiques des Réacteurs Triphasiques à Lit Fixe Fonctionnant à Co-courant vers le Bas). Ph.D. Dissertation, Institut National Polytechnique de Lorraine, Nancy, France, 1988.
- Ellman, M. J.; Midoux, N.; Laurent, A.; Charpentier, J. C. A New, Improved Pressure Drop Correlation for Trickle-Bed Reactors. *Chem. Eng. Sci.* **1988**, *43*, 2201.
- Ellman, M. J.; Midoux, N.; Wild, G.; Laurent, A.; Charpentier, J. C. A New, Improved Liquid Hold-up Correlation for Trickle-Bed Reactors. *Chem. Eng. Sci.* **1990**, *45*, 1677.
- Ergun, S. Fluid Flow through Packed Columns. *Chem. Eng. Prog.* **1952**, *48*, 89.
- Euzen, J. P.; Trambouze, P.; Wauquier, J. P. Methodology for the Scale-up of Chemical Processes (Méthodologie pour l'extrapolation des procédés chimiques). *Publications de l'Institut Français du Pétrole*; Éditions Technip Institute of French Studies: New York, 1993.
- Froment, G. F.; Depauw, G. A.; Vanrysselberghe, V. Kinetic Modelling and Reactor Simulation in Hydrodesulfurization of Oil Fractions. *Ind. Eng. Chem. Res.* **1994**, *33*, 2975.
- Germain, A. Industrial Applications of Three-Phase Catalytic Fixed Bed Reactors. In *Mass Transfer with Chemical Reaction in Multiphase Systems: Three-Phase Systems*; Alper, E., Ed.; Martinus Nijhoff Publ.: The Hague, The Netherlands, 1983; Vol. II, p 19.
- Germain, A.; L'Homme, G.; Lefebvre, A. The Trickle Flow and Bubble Flow Reactors in Chemical Processing. In *Chemical Engineering of Gas-Liquid-Solid Catalyst Reactions*; L'Homme, G. A., Ed.; CEBEDOC: Liege, Belgium, 1979; p 265.
- Gianetto, A.; Berruti, F. Modelling of Trickle-Bed Reactors. In *Chemical Reactor Design and Technology*; DeLasa, H. I., Ed.; Nijhoff: The Hague, The Netherlands, 1986; p 631.
- Gianetto, A.; Specchia, V. Trickle-Bed Reactors: State of Art and Perspectives. *Chem. Eng. Sci.* **1992**, *47*, 3197.
- Gianetto, A.; Baldi, G.; Specchia, V.; Sicardi, S. Hydrodynamics and Solid-Liquid Contacting Effectiveness in Trickle-Bed Reactors. *AIChE J.* **1978**, *24*, 1087.
- Gierman, H. Design of Laboratory Hydrotreating Reactors Scaling Down Trickle-Flow Reactors. *Appl. Catal.* **1988**, *43*, 277.
- Goto, S.; Smith, J. M. Trickle-Bed Reactor Performance. Part II: Reaction Studies. *AIChE J.* **1974**, *21*, 714.
- Goto, S.; Smith, J. M. Trickle-Bed Reactor Performance. *AIChE J.* **1975**, *21*, 706.
- Goto, S.; Mabuchi, K. Oxidation of Ethanol in Gas-Liquid Upflow and Downflow Reactors. *Can. J. Chem. Eng.* **1984**, *62*, 865.
- Goto, S.; Levec, J.; Smith, J. M. Trickle-Bed Oxidation Reactors. *Catal. Rev. Sci. Eng.* **1977**, *15*, 187.
- Grosser, K.; Carbonell, R. G.; Sundaresan, S. Onset of Pulsing in Two-Phase Cocurrent Downflow Through a Packed Bed. *AIChE J.* **1988**, *34*, 1850.
- Gupta, R. In *Handbook of Fluids in Motion*; Cheremisinoff, N. P., Gupta, R., Eds.; Ann Arbor Science: Ann Arbor, MI, 1985.
- Handley, D.; Heggs, P. J. Momentum and Heat Transfer Mechanisms in Regular Shaped Packings. *Trans. Inst. Chem. Eng.* **1968**, *46*, T251.
- Hanika, J.; Stanek, V. Operation and Design of Trickle-Bed Reactors. In *Handbook of Heat and Mass Transfer: Mass Transfer and Reactor Design*; Cheremisinoff, N. P., Ed.; Gulf Publ. Corp.: Houston, TX, 1986; Vol. 2, p 1029.
- Harold, M. P.; Watson, P. C. Bimolecular Exothermic Reaction With Vaporization in the Half-Slab Catalyst. *Chem. Eng. Sci.* **1993**, *48*, 981.
- Hartman, M.; Coughlin, R. W. Oxidation of SO₂ in Trickle-Bed Packed with Carbon. *Chem. Eng. Sci.* **1971**, *27*, 867.
- Hasseni, W.; Laurent, A.; Midoux, N.; Charpentier, J. C. Flow Regimes in Trickle Beds at High Pressure (0.1–10 MPa) (Régimes d'Écoulement dans un Réacteur Catalytique à Lit Fixe Arrosé Fonctionnant sous Pression (0.1–10 MPa) à Co-courant de Gaz et de Liquide vers le Bas). *Entropie* **1987**, *137/138*, 127.
- Haure, P. M.; Hudgins, R. R.; Silveston, P. L. Steady-State Models for SO₂ Oxidation in Trickle-Bed Reactors. *Chem. Eng. J.* **1990**, *43*, 121.
- Henry, H. C.; Gilbert, J. B. Scale-up of Pilot Plant Data for Catalytic Hydroprocessing. *Ind. Eng. Chem. Process Des. Dev.* **1973**, *12*, 328.
- Herskowitz, M.; Smith, J. M. Trickle-Bed Reactors: A Review. *AIChE J.* **1983**, *29*, 1.
- Hofmann, H. Hydrodynamics, Transport Phenomena, and Mathematical Models in Trickle-Bed Reactors. *Int. Chem. Eng.* **1977**, *17*, 19. Also in *Chem. Ing. Technol.* **1975**, *47*, 823.
- Hofmann, H. Multiphase Catalytic Packed Bed Reactors. *Catal. Rev. Sci. Eng.* **1978**, *17*, 71.
- Hofmann, H. Fluid Dynamics, Mass Transfer and Chemical Reaction in Multiphase Catalytic Fixed Bed Reactors. In *Mass Transfer with Chemical Reaction in Multiphase Systems: Three-Phase Systems*; Alper, E., Ed.; Martinus Nijhoff Publ.: The Hague, The Netherlands, 1983; Vol. II, p 73.
- Holub, R. A.; Dudukovic, M. P.; Ramachandran, P. A. A Phenomenological Model of Pressure Drop, Liquid Hold-up and Flow Regime Transition in Gas-Liquid Trickle Flow. *Chem. Eng. Sci.* **1992**, *47*, 2343–2348.
- Holub, R. A.; Dudukovic, M. P.; Ramachandran, P. A. Pressure Drop, Liquid Hold-up and Flow Regime Transition in Trickle Flow. *AIChE J.* **1993**, *39*, 302–321.
- Kawabata, J.; Yumiyama, M.; Tazaki, Y.; Honma, S.; Chiba, T.; Sumiya, T.; Endo, K. Characteristics of Gas Fluidized Beds under Pressure. *J. Chem. Eng. Jpn.* **1981**, *14*, 85–89.
- Khadilkar, M. R.; Wu, Y. X.; Al-Dahhan, M. H.; Dudukovic, M. P.; Colakyan, M. Comparison of Trickle-Bed and Upflow Reactor Performance at High Pressure: Model Predictions and Experimental Observations. *Chem. Eng. Sci.* **1996**, *51*, 2139–2148.
- Kiared, K.; Zoulalian, A. Study and Modeling of Catalytic Sulfur Dioxide Oxidation in Verlifix Three-Phase Reactor. *Chem. Eng. Sci.* **1992**, *47*, 3705–3712.
- Kohler, M.; Richarz, W. Untersuchungen des Flüssigkeitshold-up in Rieselbettreaktoren. *Chem. Eng. Technol.* **1984**, *56*, 1–19.
- Kohler, M.; Richarz, W. Investigation of Liquid Hold-up in Trickle Bed Reactors. *Ger. Chem. Eng.* **1985**, *8*, 295–300.
- Koros, R. M. Scale-up Considerations for Mixed Phase Catalytic Reactors. In *Multiphase Chemical Reactors*; Rodrigues, A. E., Calo, J. M., Sweed, N. H., Eds.; NATO Advanced Study Institute Series E; Sitjhoff & Noordhoff: Aalphen aan den Rijn, The Netherlands, 1981; Vol. 52, p 429.
- Krauze, R.; Serwinski, M. Moistened Surface and Fractional Wetted Area of Ceramic Raschig Rings. *Inz. Chem.* **1971**, *1*, 415.
- L'Air Liquide. *Encyclopédie des Gaz*; Elsevier: Amsterdam, The Netherlands, 1976.
- Larachi, F. Three-Phase Trickle and Flooded Fixed-Bed Reactors: Influence of Pressure on the Hydrodynamics and the Gas-Liquid Mass Transfer (Les Réacteurs Triphasiques à Lit Fixe à Écoulement à Co-courant vers le Bas et vers le Haut de Gaz et de Liquide. Étude de l'Influence de la Pression sur l'Hydrodynamique et le Transfert de Matière Gaz-Liquide). Ph.D. Dissertation, Institut National Polytechnique de Lorraine, Nancy, France, 1991.
- Larachi, F.; Midoux, N.; Laurent, A. Hydrodynamic Study of a Pressurized Trickle-Bed Reactor. Liquid Saturation, Single-Phase and Two-Phase Pressure Drop. In *2nd International Symposium on High Pressure Chem. Engineering*, Erlangen, Germany, Sept 24–26, 1990; Vetter G., Ed.; DECHEMA: Frankfurt, Germany, 1990; p 441.
- Larachi, F.; Laurent, A.; Midoux, N.; Wild, G. Experimental study of a Trickle-Bed Reactor Operating at High Pressure: Two-Phase Pressure Drop and Liquid Saturation. *Chem. Eng. Sci.* **1991a**, *46*, 1233.
- Larachi, F.; Laurent, A.; Wild, G.; Midoux, N. Some Experimental Liquid Saturation Results in Fixed-Bed Reactors Operated under Elevated Pressure in Cocurrent Upflow and Downflow of the Gas and the Liquid. *Ind. Eng. Chem. Res.* **1991b**, *30*, 2404.
- Larachi, F.; Laurent, A.; Midoux, N.; Wild, G. Liquid Saturation Data in Trickle Beds Operating Under Elevated Pressure. *AIChE J.* **1991c**, *37*, 1109.

- Larachi, F.; Laurent, A.; Midoux, N. Pressure Effects on the Liquid Saturation of a Trickle-Bed Reactor. *Technol. Today* **1991d**, 1, 146.
- Larachi, F.; Laurent, A.; Wild, G.; Midoux, N. Pressure Effects on Gas-Liquid Interfacial Areas in Cocurrent Trickle-Flow Reactors. *Chem. Eng. Sci.* **1992**, 47, 2325.
- Larachi, F.; Laurent, A.; Wild, G.; Midoux, N. Effect of Pressure on the Trickle-Pulsed Transition in Irrigated Fixed Bed Catalytic Reactors (Effet de la Pression sur la Transition Ruisselant-Pulsé dans les Réacteurs Catalytiques à Lit Fixe Arrosé). *Can. J. Chem. Eng.* **1993a**, 71, 319.
- Larachi, F.; Laurent, A.; Wild, G.; Midoux, N. Influence of Pressure on the Hydrodynamics of Flooded-Fixed Beds (Contribution à l'Étude de l'Influence de la Pression sur l'Hydrodynamique des Lits Fixes Noyés). *Récents Prog. Génie Procédés* **1993b**, 30, 79.
- Larachi, F.; Wild, G.; Laurent, A.; Midoux, N. Influence of Gas Density on the Hydrodynamics of Cocurrent Gas-Liquid Upflow Fixed-Bed Reactors. *Ind. Eng. Chem. Res.* **1994**, 33, 519.
- Lara-Márquez, A.; Larachi, F.; Wild, G.; Laurent, A. Mass Transfer Characteristics of Fixed Beds with Cocurrent Upflow and Downflow. A Special Reference to the Effect of Pressure. *Chem. Eng. Sci.* **1992**, 47, 3485.
- Larkins, R. P.; White, R. R.; Jeffrey, D. W. Two-Phase Cocurrent Upflow and Downflow. *AIChE J.* **1961**, 7, 231.
- Lazzaronni, C. L.; Keselman, H. R.; Figoli, H. S. Calorimetric Evaluation of the Efficiency of Liquid-Solid Contacting in Trickle Flow. *Ind. Eng. Chem. Res.* **1988**, 27, 1132.
- Lemcoff, N. O.; Cukierman, A. L.; Martinez, O. M. Effectiveness Factor of Partially Wetted Catalyst Particles: Evaluation and Application to the Modeling of Trickle Bed Reactors. *Catal. Rev. Sci. Eng.* **1988**, 30, 393.
- Levec, J.; Smith, J. M. Oxidation of Acetic Acid Solutions in a Trickle-Bed Reactor. *AIChE J.* **1976**, 22, 159.
- Levec, J.; Lakota, A. Liquid-Solid Mass Transfer in Packed Beds with Cocurrent Downward Two-Phase Flow. In *Heat and Mass Transfer in Porous Media*; Quintard, M., Todorovic, M., Eds.; Elsevier: Amsterdam, The Netherlands, 1992, p 663.
- Lockhart, R. W.; Martinelli, R. C. Proposed Correlation of Data for Isothermal Two-Phase, Two-Component Flow in Pipes. *Chem. Eng. Prog.* **1949**, 45, 39.
- Martinez, O. M.; Cassanello, M. C.; Cukierman, A. L. Three-Phase Fixed Bed Catalytic Reactors: Application to Hydrotreatment Processes. *Trends Chem. Eng.* **1994**, 2, 393.
- Mata, A. R.; Smith, J. M. Oxidation of Sulfur Oxide in Trickle-Bed Reactor. *Chem. Eng. J.* **1981**, 22, 229.
- McManus, R. L.; Funk, G. A.; Harold, M. P.; Ng, K. M. Experimental Study of Reaction in Trickle-Bed Reactors with Liquid Maldistribution. *Ind. Eng. Chem. Res.* **1993**, 32, 570.
- Mears, D. E. The Role of Axial Dispersion in Trickle Flow Laboratory Reactors. *Chem. Eng. Sci.* **1974**, 26, 1361.
- Meyers, R. A. *Handbook of Petroleum Refining Processes*, 2nd ed.; McGraw-Hill: New York, 1996.
- Midoux, N.; Favier, M.; Charpentier, J. C. Flow Pattern, Pressure Loss and Liquid Hold-up Data in Gas-Liquid Downflow Packed Beds with Foaming and Nonfoaming Hydrocarbons. *J. Chem. Eng. Jpn.* **1976**, 9, 350.
- Mills, P. L.; Dudukovic, M. P. Evaluation of Liquid-Solid Contacting in Trickle Beds by Tracer Methods. *AIChE J.* **1981**, 27, 893.
- Mills, P. L.; Dudukovic, M. P. A Comparison of Current Models for Isothermal Trickle-Bed Reactors. Application of a Model Reaction System. *ACS Symp. Ser.* **1984**, 234, 37.
- Molerus, O.; Schweintzer, J. Resistance of Particles Beds at Reynolds Numbers up to $Re \sim 10^4$. *Chem. Eng. Sci.* **1989**, 44, 1071.
- Morsi, B. I.; Laurent, A.; Midoux, N.; Barthole-Delauney, G.; Storck, A.; Charpentier, J. C. Hydrodynamics and Gas-Liquid-Solid Interfacial Parameters of Co-Current Downward Two-Phase Flow in Trickle-Bed Reactors. AIChE Annual Meeting, New Orleans, LA, Nov 8-12, 1981.
- Morsi, B. I.; Midoux, N.; Laurent, A.; Charpentier, J. C. Hydrodynamics and Interfacial Areas in Downward Cocurrent Gas-Liquid Flow Through Fixed Beds. Influence of the Nature of the Liquid. *Int. Chem. Eng.* **1982**, 22, 141.
- Nakamura, M.; Hamada, Y.; Toyama, S.; Fouda, A. E.; Capes, C. E. An Experimental Investigation of Minimum Fluidization Velocity at Elevated Temperatures and Pressures. *Can. J. Chem. Eng.* **1985**, 63, 8.
- Ng, K. M. A Model for Flow Regime Transitions in Cocurrent Downflow Trickle-Bed Reactors. *AIChE J.* **1986**, 32, 115.
- Ng, K. M.; Chu, C. F. Trickle-Bed Reactors. *Chem. Eng. Prog.* **1987**, Nov. 55.
- Olowson, P. A.; Almstedt, A. E. Influence of Pressure on the Minimum Fluidization Velocity. *Chem. Eng. Sci.* **1991**, 46, 637.
- Onda, K.; Takeuchi, H.; Kayama, Y. Effect of Packing Materials on Wetted Surface Area. *Kagaku Kogaku* **1967**, 31, 126.
- Østergaard, K. Gas-Liquid-Particle Operations in Chemical Reaction Engineering. In *Advances in Chemical Engineering*; Academic Press: Drew, T. B., Cokelet, G. R., Hoopes, J. W., Vermeulen, T., Eds.; New York, 1968; Vol. 7, p 71.
- Oyevaar, M. H.; de la Rie, T.; van der Sluijs, C. L.; Westerterp, K. R. Interfacial Areas and Gas Hold-ups in Bubble columns and Packed Bubble columns at Elevated Pressures. *Chem. Eng. Proc.* **1989**, 26, 1.
- Papayannakos, N. G.; Galtier, P. A.; Bigeard, P. H.; Kasztelan, S. Hydrodynamic Effects in Bench Scale Hydrotreaters Operating in Cocurrent Gas-Liquid Upflow Mode. *Chem. Eng. Sci.* **1992**, 47, 2275.
- Perrut, M. Flow of Supercritical Fluids Through Porous Media (Écoulement des Fluides en État Supercritique dans les Milieux Poreux). *Récents Prog. Génie Procédés* **1987**, 2, 260.
- Puranik, S. S.; Vogelpohl, V. Effective Interfacial Area in Irrigated Packed Columns. *Chem. Eng. Sci.* **1974**, 29, 501.
- Ramachandran, P. A.; Chaudhari, R. V. *Three-Phase Catalytic Reactors*; Gordon & Breach: New York, 1983.
- Ramachandran, P. A.; Dudukovic, M. P.; Mills, P. L. Recent Advances in the Analysis and Design of Trickle-Bed Reactors. *Sadhana* **1987**, 10, 269.
- Rao, V. G.; Drinkenburg, A. A. H. Solid-Liquid Mass Transfer in Packed Beds with Cocurrent Gas-Liquid Downflow. *AIChE J.* **1985**, 31, 1059.
- Reid, R. C.; Prausnitz, J. M.; Poling, B. E. *The Properties of Gases and Liquids*, 4th ed.; McGraw-Hill: New York, 1987.
- Ring, Z. E.; Missen, R. W. Trickle-Bed Reactors: Tracer Study of Liquid Hold-up and Wetting Efficiency at High Temperature and Pressure. *Can. J. Chem. Eng.* **1991**, 69, 1016.
- Rowe, P. N. The Effect of Pressure on Minimum Fluidisation Velocity. *Chem. Eng. Sci.* **1984**, 39, 173.
- Rowe, P. N.; Foscolo, P. U.; Hoffmann, A. C.; Yates, J. G. X-ray Observations of Gas-Fluidised Beds under Pressure. In *Fluidization IV*; Kunii, D., Toei, R., Eds.; Engineering Foundation: New York, 1984; p 53.
- Ruecker, C. M.; Akgerman, A. Determination of Wetting Efficiencies for a Trickle-Bed Reactor at High Temperatures and Pressures. *Ind. Eng. Chem. Res.* **1987**, 26, 164.
- Saada, M. Y. Fluid Mechanics of Cocurrent Two-Phase Flow in Packed Beds: Pressure Drop and Liquid Hold-up Studies. *Periodica Polym. Chem. Eng.* **1975**, 19, 317.
- Salatino, P.; Massimila, L. Pressure Drop in Flow of Nearly Critical Fluid through Packed Beds of Spheres. *Chem. Eng. Commun.* **1990**, 93, 101.
- Saroha, A. K.; Nigam, K. D. P. Trickle-Bed Reactors. *Reviews in Chemical Engineering*; 1996; Vol. 12, Chapters 3-4, p 207.
- Satterfield, C. N. Trickle-Bed Reactors. *AIChE J.* **1975**, 21, 209.
- Satterfield, C. N.; Way, P. F. The Role of the Liquid Phase in the Performance of a Trickle-Bed Reactor. *AIChE J.* **1972**, 18, 305.
- Satterfield, C. N.; Van Eek, M. W.; Bliss, G. S. Liquid-Solid Mass Transfer in Packed Bed with Downward Cocurrent Gas-Liquid Flow. *AIChE J.* **1978**, 24, 709.
- Saxena, S. C.; Vogel, G. J. The Properties of a Dolomite Bed of a Range of Particle Sizes and Shapes at Minimum Fluidization. *Can. J. Chem. Eng.* **1976**, 54, 453.
- Schwartz, J. G.; Weger, E.; Dudukovic, M. P. A New Tracer Method for Determination of Solid-Liquid Contacting Efficiency in Trickle-Bed Reactors. *AIChE J.* **1976**, 22, 894.
- Sebastian, H. M.; Lin, H. M.; Chao, K. C. Correlation of Solubility of Hydrogen in Hydrocarbon Solvent. *AIChE J.* **1981**, 27, 138.
- Shah, Y. T. *Gas-Liquid-Solid Reactor Design*; McGraw-Hill: New York, 1979.
- Shulman, H. L.; Ullrich, C. F.; Proulx, A. Z.; Zimmerman, J. O. Performance of Packed Column II: Wetted and Effective Interfacial Area, Gas and Liquid Mass Transfer Rates. *AIChE J.* **1955**, 1, 353.
- Sie, S. T. Scale Effects in Laboratory and Pilot-Plant Reactors for Trickle-Flow Processes. *Rev. Inst. Fr. Pet.* **1991**, 46, 501.
- Simpson, H. C.; Rodger, B. W. The Fluidization of Light Solids by Gases under Pressure and Heavy Solids by Water. *Chem. Eng. Sci.* **1961**, 16, 153.

- Specchia, V.; Baldi, G. Pressure Drop and Liquid Hold-up for Two-Phase Cocurrent Flow in Packed Beds. *Chem. Eng. Sci.* **1977**, *32*, 515.
- Specchia, V.; Baldi, G.; Gianetto, L. Solid-Liquid Mass Transfer in Cocurrent Two-Phase Flow Through Packed Beds. *Ind. Eng. Chem. Process Des. Dev.* **1978**, *17*, 362.
- Stuber, F.; Wilhelm, A. M.; Delmas, H. Modelling of Three-Phase Catalytic Upflow Reactor: A Significant Chemical Determination of Liquid-Solid and Gas-Liquid Mass Transfer Coefficients. *Chem. Eng. Sci.* **1996**, *51*, 2161.
- Sundareshan, S. Mathematical Modeling of Pulsing Flow in Large Trickle Beds. *AIChE J.* **1987**, *33*, 455.
- Tahraoui, K. Hydrodynamics, Mass Transfer, Implementation and Modeling of a Catalytic Reaction in a Three-Phase Verliflex Reactor Equipped with a Jet Venturi (Hydrodynamique, Transferts de Matière, Mise en Œuvre et Modélisation d'une Réaction Catalytique dans un Réacteur Triphase Verliflex Muni d'un Venturi à jet). Ph.D. Dissertation, Institut National Polytechnique de Lorraine, Nancy, France, 1990.
- Talmor, E. Two-Phase Downflow Through Catalyst Beds. *AIChE J.* **1977**, *23*, 868.
- Tan, C. S.; Smith, J. M. A Dynamic Method for Liquid-Particle Mass Transfer in Trickle Beds. *AIChE J.* **1982**, *28*, 190.
- Tarhan, M. O. *Catalytic Reactor Design*; McGraw-Hill: New York, 1983.
- Thanos, A. M.; Galtier, P. A.; Papayannakos, N. G. Liquid Flow Non-Idealities and Hold-Up in a Pilot Scale Packed Bed Reactor with Cocurrent Gas-Liquid Upflow. *Chem. Eng. Sci.* **1996**, *51*, 2709.
- Trambouze, P. Multiphase Catalytic Reactors in the Oil Industry, an Introduction. *Rev. Inst. Fr. Pet.* **1991**, *46*, 433.
- Trambouze, P. Engineering of Hydrotreating Processes. In *Chemical Reactor Technology for Environmentally Safe Reactors and Products*; De Lasa, H. I., Dogu, G., Ravella A., Eds.; NATO Advanced Study Institute Series E; Plenum: New York, 1993; p 425.
- Tsamatsoulis, D.; Papayannakos, N. Axial Dispersion Model and Hold-up in a Bench-Scale Trickle-Bed Reactor at Operating Conditions. *Chem. Eng. Sci.* **1994**, *49*, 523.
- Tsamatsoulis, D.; Papayannakos, N. Simulation of Non-Ideal Flow in a Trickle-Bed Hydrotreater by Crossflow Model. *Chem. Eng. Sci.* **1995**, *50*, 3685.
- Turek, F.; Lange, R. Mass Transfer in Trickle-Bed Reactors at Low Reynolds Number. *Chem. Eng. Sci.* **1981**, *36*, 569-579.
- Van de Vusse, J. G.; Wesselingh, J. A. Multiphase Reactors. *Proceedings of the 4th International/6th European Symposium on Chemical Reaction Engineering*; VDI: Heidelberg, Germany, 1976.
- van Gelder, K. B.; Westerterp, K. R. Residence Time Distribution and Hold-up in a Co-current Upflow Packed Bed Reactor at Elevated Pressure. *Chem. Eng. Technol.* **1990**, *13*, 27-40.
- Van Klinken, J.; Van Dongen, R. H. Catalyst Dilution for Improved Performance of Laboratory Trickle-Flow Reactors. *Chem. Eng. Sci.* **1980**, *35*, 59.
- Van Landeghem, H. Multiphase Reactors: Mass Transfer and Modeling. *Chem. Eng. Sci.* **1980**, *35*, 1912-1949.
- Vanrysselberghe, V.; Froment, G. F. Hydrodesulfurization of Dibenzothiophene on CoMo/Al₂O₃ Catalyst: Reaction Network and Kinetics. *Ind. Eng. Chem. Res.* **1996**, *35*, 3311-3318.
- Vergel, H. C. A. Gas-Liquid Catalytic Fixed Bed Reactors. Experimental and Theoretical Comparison of the Performances of the Reactor for Different Flow Directions (Les Réacteurs Catalytiques à Lit Fixe avec Écoulement de Gaz et de Liquide. Comparaison sur le Plan Théorique et Expérimental de la Performance du Réacteur dans Différents Sens d'Écoulement). Ph.D. Dissertation, Institut National Polytechnique de Lorraine, Nancy, France, 1993.
- Vergel, H. C. A.; Euzen, J. P.; Trambouze, P.; Wauquier, J. P. Two-Phase Flow Catalytic Reactor. Influence of Hydrodynamics on Selectivity. *Chem. Eng. Sci.* **1995**, *50*, 3303.
- Wammes, W. J. A. Hydrodynamics in cocurrent gas-liquid trickle-bed reactor at elevated pressure. Ph.D. Thesis, University of Twente, Enschede, The Netherlands, 1990.
- Wammes, W. J. A.; Westerterp, K. R. Hydrodynamics in a Cocurrent Gas-Liquid Trickle-Bed Reactor at Elevated Pressures. In *2nd International Symposium on High Pressure Chemical Engineering*, Erlangen, Germany, Sept 24-26, 1990; Vetter, G., Ed.; DECHEMA: Frankfurt, Germany, 1990; p 435.
- Wammes, W. J. A.; Westerterp, K. R. Hydrodynamics in a Pressurized Cocurrent Gas-Liquid Trickle-Bed Reactor. *Chem. Eng. Technol.* **1991**, *14*, 406.
- Wammes, W. J. A.; Mechielsen, S. J.; Westerterp, K. R. The Transition Between Trickle Flow and Pulse Flow in a Cocurrent Gas-Liquid Trickle-Bed Reactor at Elevated Pressures. *Chem. Eng. Sci.* **1990a**, *45*, 3149.
- Wammes, W. J. A.; Mechielsen, S. J.; Westerterp, K. R. The Influence of the Reactor Pressure on the Hydrodynamics in a Cocurrent Gas-Liquid Trickle-Bed Reactor. *Chem. Eng. Sci.* **1990b**, *45*, 2247.
- Wammes, W. J. A.; Mechielsen, S. J.; Westerterp, K. R. The Influence of Pressure on the Liquid Hold-up in a Cocurrent Gas-Liquid Trickle-Bed Reactor Operating at low Gas Velocities. *Chem. Eng. Sci.* **1991a**, *46*, 409.
- Wammes, W. J. A.; Middelkamp, J.; Huisman, W. J.; de Baas, C. M.; Westerterp, K. R. Hydrodynamics in a Cocurrent Gas-Liquid Trickle Bed at Elevated Pressures. *AIChE J.* **1991b**, *37*, 1849.
- Weekman, V. W. Hydroprocessing Reaction Engineering. In *Proceedings of the 4th International/6th European Symposium on Chemical Reaction Engineering*; VDI: Heidelberg, Germany, 1976.
- Wild, G.; Larachi, F.; Laurent, A. The Hydrodynamic Characteristics of Cocurrent Downflow and Cocurrent Upflow Gas-Liquid-Solid Catalytic Fixed Bed Reactors: The Effect of Pressure. *Rev. Inst. Fr. Pet.* **1991**, *46*, 467.
- Wild, G.; Larachi, F.; Charpentier, J. C. Heat and Mass Transfer in Gas-Liquid-Solid Fixed Bed Reactors. In *Heat and Mass Transfer in Porous Media*; Quintard M., Todorovic, M., Eds.; Elsevier: Amsterdam, The Netherlands, 1992; p 616.
- Wu, Y.; Khadilkar, M. R.; Al-Dahhan, M. H.; Dudukovic, M. P. Comparison of Upflow and Downflow Two-Phase Flow Packed-Bed Reactors with and without Fines: Experimental Observations. *Ind. Eng. Chem. Res.* **1996a**, *35*, 397.
- Wu, Y.; Al-Dahhan, M. A.; Khadilkar, M. R.; Dudukovic, M. P. Evaluation of Trickle Bed Reactor Models for a Liquid Limited Reaction. *Chem. Eng. Sci.* **1996b**, *51*, 2721.
- Zhukova, T.; Pisarenko, B. V. N.; Kafarov, V. V. Modeling and Design of Industrial Reactors with a Stationary Bed of Catalyst and Two-Phase Gas-Liquid Flow—A Review. *Int. Chem. Eng.* **1990**, *30*, 57.

Received for review January 29, 1997
 Revised manuscript received April 23, 1997
 Accepted April 24, 1997*

IE9700829

* Abstract published in *Advance ACS Abstracts*, July 1, 1997.